**AD**_____

**Award Number:** W81XWH-09-1-0314

**TITLE:** Molecular targeting of prostate cancer during androgen ablation: inhibition of CHES1/FOXN3

**PRINCIPAL INVESTIGATOR:** Clifford G. Tepper, Ph.D.

**CONTRACTING ORGANIZATION:** University of California, Davis
Davis, CA 95618-6134

**REPORT DATE:** May 2010

**TYPE OF REPORT:** Annual

**PREPARED FOR:** U.S. Army Medical Research and Materiel Command
Fort Detrick, Maryland 21702-5012

**DISTRIBUTION STATEMENT:**

- ✓ Approved for public release; distribution unlimited

# REPORT DOCUMENTATION PAGE

*Form Approved*
*OMB No. 0704-0188*



**PLEASE DO NOT RETURN YOUR FORM TO THE ABOVE ADDRESS.**

| 1. REPORT DATE *(DD-MM-YYYY)* | 2. REPORT TYPE | 3. DATES COVERED *(From - To)* |
|---|---|---|
| 10-05-2010 | Annual | 15 APR 2009 - 14 APR 2010 |

**4. TITLE AND SUBTITLE**

Molecular targeting of prostate cancer during androgen ablation: inhibition of CHES1/FOXN3

**5a. CONTRACT NUMBER**

W81XWH-09-01-0314

**5b. GRANT NUMBER**

PC081032

**5c. PROGRAM ELEMENT NUMBER**

**6. AUTHOR(S)**

Tepper, Clifford G.

Email: cgtepper@ucdavis.edu

**5d. PROJECT NUMBER**

**5e. TASK NUMBER**

**5f. WORK UNIT NUMBER**

**7. PERFORMING ORGANIZATION NAME(S) AND ADDRESS(ES)**

University of California, Davis
Davis, CA 95618-6134

**8. PERFORMING ORGANIZATION REPORT NUMBER**

**9. SPONSORING/MONITORING AGENCY NAME(S) AND ADDRESS(ES)**

U.S. Army Medical Research and Materiel Command
Fort Detrick, Maryland 21702-5012

**10. SPONSOR/MONITOR'S ACRONYM(S)**

**11. SPONSOR/MONITOR'S REPORT NUMBER(S)**

**12. DISTRIBUTION/AVAILABILITY STATEMENT**

Approved for public release; distribution unlimited

**13. SUPPLEMENTARY NOTES**

**14. ABSTRACT**

Our operating hypothesis is that checkpoint suppressor 1 (CHES1)/FOXN3 is an androgen withdrawal-induced gene that promotes prostate cancer resistance to apoptosis. The purposes of this research are two-fold. The first is to define the mechanisms of CHES1 gene expression regulation and function, particularly in mediating apoptosis resistance during androgen ablation. Secondly, the tools yielded from our functional studies will be utilized to test the efficacy of CHES1-silencing therapy (CST) in preventing castration-resistant prostate cancer and to develop a mechanism-based noninvasive imaging strategy for monitoring the success of CST. Several significant findings were made. Of major clinical importance, CHES1 expression was elevated substantially during combined androgen blockade and was associated with enhanced PI3K/Akt activation and suppression of pro-apoptotic BNIP3 expression. Conversely, CHES1 down-regulation is potentially necessary for genotoxic stress to trigger apoptosis. To test the hypothesis that CHES1 could be exploited as a therapeutic target, we developed and validated several LNCaP sublines in which we can conditionally silence CHES1 expression, thereby providing us with the necessary models to easily test the value of potential CST

**15. SUBJECT TERMS**

Prostate cancer, androgen receptor, hormonal therapy, forkhead, apoptosis, chemotherapy, RNA interference, imaging

| 16. SECURITY CLASSIFICATION OF: | | | 17. LIMITATION OF ABSTRACT | 18. NUMBER OF PAGES | 19a. NAME OF RESPONSIBLE PERSON |
|---|---|---|---|---|---|
| a. REPORT | b. ABSTRACT | c. THIS PAGE | | | USAMRMC |
| U | U | U | UU | 51 | 19b. TELEPHONE NUMBER *(Include area code)* |

## Table of Contents

**Page**

## INTRODUCTION

Androgen is a pivotal mediator of the growth, survival, and differentiation of prostate cancer (CaP) cells. Accordingly, androgen ablation is the first-line therapy for metastatic disease and dependably mediates disease regression. Unfortunately, this treatment is only palliative, as the disease typically recurs as castration-resistant prostate cancer (CRPC) approximately two years later and accounts for the 20% mortality rate due to this neoplasm. Therefore, defining the mechanisms underlying CaP survival during androgen withdrawal (AW) and the establishment of castration resistance are critical to enhancing our understanding of disease progression and the development of more efficacious therapies. We identified *FOXN3*/*CHES1* (*Checkpoint suppressor 1*) as a potential molecular mediator of CaP survival during androgen ablation. Our findings demonstrated that *CHES1* exhibits an AW-induced expression pattern and is an anti-apoptotic molecule that potentially acts via induction of the phosphatidylinositol 3-kinase (PI3K)/Akt pathway and/or down-regulation of the pro-apoptotic Bcl-2 family members *BNIP3* and *BAK1*. Importantly, antagonism of its function by RNA interference (RNAi)-mediated silencing resulted in apoptotic cell death of LNCaP cells selectively in the absence of androgen. That being said, ***the operating hypothesis of this work is that CHES1 is an AW-induced gene that functions to promote prostate cancer resistance to apoptosis and can be exploited as a therapeutic target.*** Therefore, there are two general purposes of this research. The first is to achieve a better understanding of mechanisms of *CHES1* gene expression regulation and function, particularly with respect to its role in mediating apoptosis resistance during androgen ablation. Secondly, the knowledge and tools yielded from our functional studies will be utilized to test the efficacy of *CHES1*-silencing therapy (CST) in preventing the emergence of CRPC and to develop a mechanism-based non-invasive imaging strategy for monitoring the success of the therapy.

## BODY

This has been the first year of funding for this proposal and I am very enthusiastically writing this report based upon the results from the work performed. Our team has been able to confirm preliminary findings described in the original grant proposal and more importantly, extend these along the lines of that described in our *Specific Aims* and the *Statement of Work*. These will be described in detail below and in the *Supporting Data* section of this report. In addition, we have included a copy of the manuscript (*Appendix*) which we plan to submit to Cancer Research in June, 2010 (1).

### Kinetics of *CHES1* and apoptosis-associated gene expression changes triggered by androgen ablation. (Task 3)

Our microarray profiling studies identified *CHES1*/*FOXN3* as an AW-induced gene in LNCaP cells. Subsequent experiments demonstrated that its expression was required for cell survival during androgen ablation and suggested that CHES1 function might antagonize apoptosis via the suppression of pro-apoptotic genes such as *BNIP3* and *BAK1*. The latter notion is certainly possible based upon its function as a transcriptional repressor (2). The experiments described in this section were designed to accomplish **Task 3**. In an effort to better define resistance mechanisms operating during androgen ablation, it is critical to perform experiments which will specifically address the different types of this therapy, including *1)* androgen withdrawal (or deprivation; **Task 3a**) and *2)* combined androgen blockade (CAB; **Task 3b**) in which AW is combined with an anti-androgen to antagonize AR activity stimulated by residual androgens. Molecular and biochemical analyses by quantitative RT-PCR (qRT-PCR) and immunoblot analyses, respectively, were performed to evaluate the expression of

*CHES1*, *BNIP3*, *BAK1*, and other molecules relevant to this context. After 96 hours of androgen deprivation, *CHES1* expression increased 4.73-fold relative to that found in cells cultured in the presence of 5$\alpha$-dihydrotestosterone (DHT) **(Fig. 1)**. While this was consistent with our microarray findings, *CHES1* levels continued to climb for the remainder of the experiment, reaching 18.2-fold at day 7. In order to investigate this phenomenon in another model and determine its relevance to tumor biology, *CHES1* expression was examined in CWR22 xenografts grown in intact or castrated nude mice. In this system, *CHES1* was up-regulated 6.15-fold at 14 days post-castration **(Fig. 2A)**. While the phenomenon is certainly similar to that of LNCaP cells, the differences in kinetics and magnitude could result from a lag in the complete removal of circulating and/or intra-prostatic androgen from the mouse as well as the complex environment of the tumor. In addition, *BNIP3* levels were reduced by 32-75% while *BAK1* steadily increased 4.88-fold **(Fig. 2B)**.

A vital part of **Task 3** was to determine if CHES1 protein levels also increase during AW. Towards this goal we tested several commercially-available CHES1 antibodies. While two of the antibodies failed to pick up any signal, the antibody purchased from Abcam (catalog # ab26158) was superb. Moreover, this enabled us to confirm that CHES1 protein levels progressively increased following the shift to AW medium **(Fig. 3)**. As expected, AR levels were diminished during AW **(Fig. 4)**. Examination of apoptosis regulatory molecules demonstrated that BNIP3 levels exhibited a more dramatic down-regulation than its transcript **(Fig. 2B, 4)** and levels of Ser473-phosphorylated Akt were greatly increased. These results suggest the establishment of an anti-apoptotic cellular context. Interestingly, while the *BNIP3* transcript and protein data are somewhat paradoxical, this acute response of BNIP3 could be mediated via miRNA action similar to that described for BAK1 (3).

Combined androgen blockade (CAB) is the first-line therapy used for the treatment of metastatic CaP. To simulate this *in vitro*, LNCaP cells were subjected to AW (3 days) and then treated with the antiandrogen bicalutamide (also called Casodex; CDX) **(Fig. 5)**. This experimented yielded very interesting, and potentially important, results. As expected, AR was highly expressed in cells cultured in the presence of DHT while CHES1 was only moderately expressed. In contrast, high-dose CDX (25 μM) down-regulated the AR, which was accompanied by elevated CHES1 expression. Interestingly, treatment with an intermediate concentration of CDX (10 μM) mediated dramatic AR stabilization after 2 days and persisted for at least 4 days. Support for this phenomenon as being *bona fide* AR stimulation is provided by the fact that CHES1 expression was repressed. To the best of our knowledge, although CDX-mediated AR activation is commonly observed indirectly in the clinic as PSA biochemical failure, it is not commonly reported in experimental systems (4, 5). It is also interesting to note that since this simulates the partial reinstatement of the AR pathway characteristic of CRPC, this agrees with our earlier data in which *CHES1* expression was reduced in androgen-independent (AI) LNCaP sublines (1).

The same experiment was performed in CWR22Pc, which is the first cell line to be derived from the androgen-dependent CWR22 xenograft (6). Although the results are more difficult to interpret than that obtained with LNCaP, there does seem to be several apparent trends **(Fig. 6B)**. First, CHES1 expression was induced under all conditions (*e.g.*, AW, CDX, etc.) in which growth or AR activity were not as robust as compared to cells grown under normal culture conditions (*i.e.*, medium supplemented with whole serum; WS, lane 1). In accord, there was an inverse association with BNIP3 expression under the same conditions. In this instance, it is worth noting that although addition of DHT to AW medium robustly stimulates the AR and prevents neuroendocrine differentiation (NED), it does not restore a growth rate equivalent to that stimulated by WS.

**Define the regulation of *CHES1* expression by p53-activating agents. (Task 6)**

Based upon the results of our experiments and data in the literature, we hypothesize that *CHES1* down-regulation is a necessary event for the propagation of specific pro-apoptotic stimuli. In this section, we want to investigate the possibility that *CHES1* is regulated by genotoxic agents, including ionizing radiation (IR), mitomycin C (MMC), and adriamycin (Adr). Our initial studies with IR demonstrated that *CHES1* was rapidly and potently repressed by IR and that this occurred coincidently with p53 activation and transcriptional induction of CDKN1A (1). Combined with the fact the *CHES1* proximal promoter contains a half-site for p53 binding, we are close to completing **Task 6c** by demonstrating that *CHES1* repression is an immediate-early response to p53 activation.

This is being further pursued using MMC and Adr, which are known to induce DNA damage and a potent p53 response. Dose-response and time-course experiments using MTS assays were performed in order to correlate the effects of treatments with growth inhibition and/or apoptosis **(Task 6a)**. These were then followed up with experiments to examine the expression of CHES1, phospho-p53 (Ser15), total p53, and other markers indicative of p53 activation (*e.g.*, MDM2) and apoptosis (*e.g.*, PARP cleavage, caspase-3) **(Task 6b)**. For these, both LNCaP and CWR22Pc cells were treated with MMC at concentrations from 0-10 µg/ml for 24 hours **(Fig. 7)**. In LNCaP, the lowest dose of MMC (0.1 µg/ml) was capable of inducing p53 activation and CHES1 down-regulation. However, only the highest dose of MMC was capable of mediating apoptosis as indicated by PARP cleavage. The association between p53 induction, CHES1 repression, and apoptosis is nicely demonstrated in the time-course experiment depicted in **Fig. 8**. In contrast, MMC did not induce apoptosis of CWR22Pc cells. Although p53 activation occurred (phospho-p53 levels were increased, p53 levels stabilized, and MDM2 expression increased), CHES1 expression was not down-regulated. Taken, together, these results suggest that a mechanism associated with CHES1 down-regulation is necessary for apoptosis to occur in response to treatment with genotoxic agents.

**Development of model systems having conditional expression or silencing of *CHES1*/*FOXN3*.**

One of the primary goals of this proposal is to better characterize the apoptotic process induced by inhibiting CHES1 function and to determine if suppression of CHES1 *in vivo* will delay the emergence of AI tumors. While the utilization of synthetic siRNA to transiently knock down CHES1 has provided excited results (1), it can be difficult to dissect signaling mechanisms set against the dynamic background established by AW. Since this includes induced expression of endogenous *CHES1*, we feel the development of tetracycline (Tet)-inducible shRNA **(Tasks 2, 4, and 5)** and cDNA **(Tasks 1, 5)** expression models is central to the success of this grant. These will be discussed separately in the sections below.

**Development of tetracycline-inducible *CHES1* expression model systems.**

A required component for this task was to also generate tetracycline-regulated LNCaP and CWR22Pc cell lines **(Task 5)**. These have been established by retroviral gene transfer of pRevTet-on. Stable pools have been selected and are currently being characterized for levels of inducibility. However, we have been delayed in completing the generation of the inducible *CHES1* expression cell lines **(Task 1)** due to a problem with the pRevTRE-HA-CHES1 expression constructs. Although we have confirmed that *CHES1* was cloned in-frame with the HA epitope tag, we cannot detect expression in pilot co-transfection (pRevTet-On + pRevTRE-HA-CHES1 + Dox) experiments performed to validate their function. As initial troubleshooting measures, we plan to utilize a different vector encoding the Tet transactivator and perform the experiment in a different cell line. If neither of these is successful, we will consider cloning the

CHES1 CDS again. In the meantime, we have started to use our constitutively-expressing LNCaP-HA-CHES1 and LNCaP-CHES1-*myc* cell lines (1). Although these are not perfect model systems, they can be valuable for selected applications.

**Development of tetracycline-inducible shRNA expression model systems.**

This aspect of the project has been quite successful. To accomplish this, **Tasks 2 and 4** were first performed in order to identify the most potent *CHES1*-specific hairpins (shRNAs) and then to move them into the tetracycline (Tet)/doxycycline (Dox)-inducible lentiviral expression vector pTRIPZ (Open Biosystems). Two strategies were used to obtain the most potent shRNA constructs. As described in the grant proposal, we utilized the pSM2 expression vector, which enables the cloned shRNA to enter the endogenous cellular RNA interference processing machinery more efficiently by virtue of being expressed in the context of a naturally-occurring miRNA (miR-30). Since large-scale shRNA libraries have already been developed in pSM2, we obtained 6 *CHES1*-specific constructs from Open Biosystems. All of these target sites in the 3'-UTR. Since these might have a tendency to mediate translational suppression, we also generated constructs with custom-designed shRNAs that have target sites within the *CHES1* CDS and potentially would lead to mRNA decay. The locations of the shRNA target sites are depicted in **Fig. 9A** and specific information for each shRNA construct are presented in **Fig. 9B**.

In order to test the *CHES1*-silencing capacity of each construct, retrovirus stocks were generated and then used to infect LNCaP cells. Stable LNCaP-pSM2-*CHES1*-Ri and vector control sublines were selected by culture in puromycin-containing medium. Subsequently, each subline was subjected to AW for 7 days followed by qRT-PCR analysis for the expression of *CHES1* **(Fig. 10)**. As shown, AW induced *CHES1* expression approximately 17-fold in the LNCaP-pSM2 empty vector control cells. In contrast, AW-induced and/or basal (*i.e.*, pSM2/+DHT) *CHES1* expression was effectively repressed in the LNCaP-pSM2-CHES1-Ri lines #1, 3, and 5.

The corresponding shRNA constructs were therefore chosen for use in the generation of the Tet-inducible shRNA constructs and cell lines **(Task 5a)**. For this, the shRNA cassette in pSM2 was subcloned into the pTRIPZ lentivector, which contains the Tet-responsive RNA Polymerase II promoter and encodes the reverse tetracycline transactivator. The methods for generating LNCaP-*tet*-*CHES1*-Ri cell lines are described in the legend to **Fig. 11**. **Task 5b** was performed in order to accomplish the establishment of stable cell lines and for validation of Dox-regulated shRNA expression and *CHES1* suppression. This experiment is described in Fig. 11 and demonstrated that in the absence of Dox, all of the LNCaP-*tet*-CHES1-Ri sublines exhibited the expected AW-inducible *CHES1* expression. In the presence of Dox, only LNCaP-*tet*-CHES1-Ri-1 and -3 exhibited repression of basal and AW-induced *CHES1* expression. Therefore, LNCaP-pTRIPZ and LNCaP-tet-CHES1-Ri-1- and -3 will be used for the subsequent studies, including those described in **Tasks 8 and 9**.

**KEY RESEARCH ACCOMPLISHMENTS**

- Confirmed that induction of CHES1/FOXN3 expression (transcript and protein) is a general feature of androgen ablation in multiple prostate cancer models *in vitro* and *in vivo*.
- Demonstrated that combined androgen blockade induces CHES1 expression more highly than androgen deprivation alone. This effect was most likely mediated by bicalutamide (Casodex).
- Demonstrated that non-inhibitory concentrations of Casodex can stabilize the AR and super-induce its expression.

- Confirmed that CHES1 is rapidly down-regulated in response to several genotoxic agents (IR, MMC, Adr) and might be the target of p53-mediated repression.
- Generated and functionally validated multiple LNCaP cell lines having constitutive or tetracycline-inducible expression of *CHES1*-targeting shRNAs.

## REPORTABLE OUTCOMES

### 1. Manuscripts

As mentioned above, we have very nearly completed writing our manuscript entitled "*Identification of checkpoint suppressor 1 (CHES1)/FOXN3 as an androgen withdrawal-induced gene mediating neuroendocrine differentiation and survival of prostate cancer cells*," which we anticipate submitting in June, 2010 (1). This has also been included as an Appendix in this report (1).

### 2. Development of expression vectors and cell lines

During this past year of funding, we have generated a number of expression constructs and LNCaP sublines. These are listed below:

a) *CHES1* RNA interference (RNAi, Ri) expression constructs:
   1. Constitutively expressed shRNA vectors: pSM2-*CHES1*-Ri-1, -2, and -3 **(Fig. 9)**.
   2. Tetracycline/doxycycline-inducible shRNA expression constructs: pTRIPZ-CHES1-Ri-1, -3, and -5 **(Fig. 11)**.

b) Tetracycline/doxycycline-inducible *CHES1* expression construct: pRev-TRE-HA-*CHES1*.

c) Stable LNCaP cell lines with constitutive expression of *CHES1* shRNAs: LNCaP-CHES1-Ri-1 through -9 **(Fig. 9)** and LNCaP-pSM2 vector control.

d) LNCaP cells with Tet/Dox-inducible *CHES1*-targeting shRNA expression: LNCaP-*tet*-CHES1-Ri-1, -3, and -5 **(Fig. 11)** and LNCaP-pTRIPZ empty vector control.

### 3. Employment opportunities

Thankfully, the funding from this proposal has provided employment and training for two individuals, in addition to myself. Dr. Nong Xiang is an extremely talented postdoctoral fellow/Associate Research Specialist who works on this project. She came to the UC Davis Cancer Center from the University of Wisconsin-Madison where she had close to seven years of experience in the prostate cancer field, which was accompanied by a significant record of productivity. Mr. Hassen Ali is a research associate in my laboratory and I was very happy to be able to have him join our *CHES1* research team. He is a graduate of UC Davis and having trained him in cellular, molecular, and biochemical techniques for close to two years in my collaborator's laboratory, I was very confident that he would be able to contribute greatly to this project.

## CONCLUSION

From the work of this past year, we can provide a summary of our key findings and make several conclusions. Our preliminary findings had demonstrated that *CHES1* was an androgen withdrawal-induced gene that mediated CaP survival by potentially functioning as an anti-apoptotic transcription factor. We have now confirmed, quantitated, and better defined all of our preliminary results that demonstrated AW-induced *CHES1* gene expression in LNCaP cells and CWR22 xenograft tumors *in vivo*. One conclusion that can be made is that elevated *CHES1* gene expression is very likely to translate to a functional outcome since we also observed that CHES1 protein levels also increase markedly. A major, clinically-relevant conclusion we can now make is that *CHES1* expression is up-regulated substantially when cells are subjected to combined androgen blockade in which an anti-androgen (*e.g.*,

bicalutamide/Cdx) is combined with androgen deprivation. If this phenomenon occurs in clinical prostate cancers, this might prove to be a significant mechanism responsible for CaP resistance to this therapy. Conversely, we also conclude that *CHES1* down-regulation accompanies, and might be a necessary event, for genotoxic stress to trigger apoptosis. Our results taken together with findings from several other groups, suggest that CHES1 could be exploited as a therapeutic target. To test this hypothesis, we developed LNCaP sublines in which we can conditionally silence *CHES1* expression, thereby providing us with the necessary models to easily test the value of a potential *CHES1*-silencing therapy (CST). In the next year, we will *1)* test the efficacy of CST to heighten cell killing during androgen ablation and in response to chemotherapeutic agents and *2)* to better understand why heightened CHES1 expression leads to resistance to apoptosis.

**REFERENCES**


1. Xiang N, Yang JK, Webb JW, et al. Identification of *checkpoint suppressor 1* (*CHES1*)/FOXN3 as an androgen withdrawal-induced gene mediating neuroendocrine differentiation and survival of prostate cancer cells. Cancer Res Submission in June, 2010.
2. Scott KL, Plon SE. CHES1/FOXN3 interacts with Ski-interacting protein and acts as a transcriptional repressor. Gene 2005; 359: 119-26.
3. Shi XB, Xue L, Yang J, et al. An androgen-regulated miRNA suppresses Bak1 expression and induces androgen-independent growth of prostate cancer cells. Proc Natl Acad Sci U S A 2007; 104: 19983-8.
4. Ishikura N, Kawata H, Nishimoto A, Nakamura R, Ishii N, Aoki Y. Establishment and characterization of an androgen receptor-dependent, androgen-independent human prostate cancer cell line, LNCaP-CS10. Prostate 2010; 70: 457-66.
5. Zhu P, Baek SH, Bourk EM, et al. Macrophage/cancer cell interactions mediate hormone resistance by a nuclear receptor derepression pathway. Cell 2006; 124: 615-29.
6. Dagvadorj A, Tan SH, Liao Z, Cavalli LR, Haddad BR, Nevalainen MT. Androgen-regulated and highly tumorigenic human prostate cancer cell line established from a transplantable primary CWR22 tumor. Clin Cancer Res 2008; 14: 6062-72.

## APPENDICES

1. Manuscript in Preparation:
   Identification of *checkpoint suppressor 1* (*CHES1*)/*FOXN3* as an androgen withdrawal-induced gene mediating neuroendocrine differentiation and survival of prostate cancer cells. N. Xiang, J. K. Yang, J. M. Webb, C. B. Wee, D. L. Boucher, S. Y. Liu, C. A. Baron, R. W. de Vere White, J. P. Gregg, H. J. Kung, and C. G. Tepper

# Identification of *checkpoint suppressor* 1 (*CHES1*)/FOXN3 as an androgen withdrawal-induced gene mediating neuroendocrine differentiation and survival of prostate cancer cells.

Nong Xiang[1], Jade K. Yang[2], John M. Webb[2], Christopher B. Wee[2], David L. Boucher[2], Stephenie Y. Liu[3], Colin A. Baron[3], Ralph W. de Vere White[1,4], Jeffrey P. Gregg[3], and Hsing-Jien Kung[1,2], and Clifford G. Tepper[1,2]

Departments of [1]Biochemistry and Molecular Medicine, [3]Pathology and Laboratory Medicine, and [4]Urology, University of California, Davis School of Medicine and [2]Division of Basic Sciences, UC Davis Cancer Center and Sacramento, CA 95817

**Running Title:** *CHES1* promotes NED and survival of prostate cancer

**Key words:** microarray, androgen independence, *CHES1*, neuroendocrine differentiation, apoptosis, RNA interference

---

**Grant support:** Support for these studies was provided by U.S. Department of Defense (DoD) grant W81XWH-09-01-0314 (C.G.T.), California Cancer Research Program grant 00-00792V-20164 (C.G.T.), and seed funding from the UC Davis Cancer Center. Microarray analysis was performed by the UC Davis Cancer Center Genomics and Expression Resource supported by Cancer Center Support Grant P30 CA93373-01 (R.W.dV.W.) from the NCI.

**Requests for reprints:** Clifford G. Tepper, University of California Davis Medical Center, Research III, Room 2200A, 4645 2nd Avenue, Sacramento, CA 95817. Phone: (916) 703-0365; Fax: (916) 734-2589; E-mail: cgtepper@ucdavis.edu.

**ABSTRACT**

The molecular mechanisms underlying the development of prostate cancer (CaP) resistance to androgen-ablative therapy are intensely studied. We performed expression profiling of androgen-deprived LNCaP cells in order to identify genes vital to the survival and eventual outgrowth of cells challenged by androgen ablation. Hierarchical clustering of the microarray data organized 159 differentially expressed genes into two clusters of androgen withdrawal (AW)-repressed and AW-induced genes. *Checkpoint suppressor 1* (*CHES1*) was identified in the latter cluster as having low expression in the presence of androgen, but marked induction (3.25-fold) following 96 hours of androgen withdrawal. *CHES1* is a forkhead transcription factor discovered in a yeast screen for potential human DNA damage checkpoint genes. However, its expression was strongly repressed by ionizing radiation-induced p53 activation. RNA interference-mediated *CHES1* silencing inhibited the basal growth of LNCaP cells and induced apoptosis in the absence of androgen. LNCaP sublines stably expressing physiologically relevant levels of the HA-tagged CHES1 protein (LNCaP-*CHES1*) were also generated. These possessed a distinctive neuroendocrine (NE) phenotype, evidenced by rounded cell bodies and extension of neuritic processes, and proliferated at an attenuated rate compared to LNCaP-*vector* cells. Biochemical characterization of LNCaP-*CHES1* cells demonstrated nuclear-localized expression of CHES1, diminished androgen receptor (AR) expression, elevated phosphorylated Akt levels, and increased neuron-specific enolase levels. In summary, our results demonstrate that *CHES1* is an AW-induced gene that promotes CaP survival in the absence of androgen and is a potential, dominant mediator of the androgen-ablated phenotype by suppressing AR signaling and promoting NE differentiation.

## INTRODUCTION

Androgen ablation is the first-line therapy for metastatic, hormone-dependent prostate cancer (CaP) and exploits the obligatory role of testicular androgens for the proliferation, differentiation, and survival of nonmalignant prostatic exocrine epithelial cells as well as cancers. This is only palliative, as hormone-refractory, or androgen-independent (AI), disease typically recurs after eighteen to twenty-four months and accounts for the 20% mortality rate due to this neoplasm (1). As a result, the mechanisms underlying the transition from androgen dependence to androgen independence are the subject of intense investigations.

The LNCaP androgen-dependent prostate carcinoma cell line has been valuable for studying the action of androgen and modeling human CaP *in vitro* and *in vivo*. Key consequences of androgen ablation in this model are AR pathway inactivation, growth arrest, neuroendocrine differentiation (NED) (2), and the engagement of mechanisms antagonizing apoptosis (3). The androgen receptor (AR) acts as the pivotal effector of androgen deprivation. Removal of its ligand simultaneously decreases AR-mediated transcriptional regulation and effectively eliminates the AR pathway by triggering a marked reduction in AR protein levels (4) via destabilization (5) and proteasome-mediated degradation (6). As a result, growth arrest rapidly ensues and is highlighted by Rb-mediated accumulation of cells in G1 and a corresponding, dramatic reduction in S-phase cells undergoing DNA replication (7).

Neuroendocrine transdifferentiation occurs simultaneously with growth arrest and is an obvious feature of androgen-deprived LNCaP cultures by virtue of striking morphological changes (2, 3). The role of androgen signaling in actively repressing NED has been supported by the ability of RNA interference (RNAi)-mediated AR gene silencing to induce phenotypic and biochemical markers of NED (8). These cells possess numerous secretory granules containing a variety of neurotrophic factors including chromogranin A, neuron-specific enolase (NSE), neurotensin, serotonin, somatostatin, and gastrin-releasing peptide/bombesin (9). While nonmalignant NE cells are normally present in the epithelium of the prostate gland, many studies have underscored the critical role of transdifferentiated, malignant NE cells and their products in mediating tumor progression via the ability to promote survival, androgen-independent proliferation, AR activation, and metastasis (9, 10).

The phosphatidylinositol 3-kinase (PI3K)/Akt pathway is a dominant survival factor for LNCaP cells during androgen deprivation. PI3K signaling is deregulated in this model due to mutational inactivation of the PTEN lipid phosphatase and a consequential accumulation of 3-phosphorylated phosphatidyl inositides. Androgen withdrawal hyperactivates the pathway and its inhibition by pharmacological inhibitors (*e.g.*, LY294002, wortmannin) or ectopic PTEN expression induced apoptosis specifically under these conditions (3, 11). Downstream anti-apoptotic mechanisms of PI3K/Akt signaling include Akt-mediated inhibition of FKHR/FKHRL1 transcription of pro-apoptotic genes and activation of mammalian target of rapamycin (mTOR) and hypoxia-inducible factor-1$\alpha$ (HIF-1$\alpha$) target genes (12). Additionally, transcriptional activation of Bcl-2 by NF-$\kappa$B and cAMP-response element-binding protein (CREB) has been linked to the PI3K pathway (13, 14). Notably, AI LNCaP sublines selected by outgrowth in hormone-free medium are characterized by elevated Bcl-2 expression (15, 16).

Genome-wide expression profiling (*e.g.*, SAGE, microarray) has contributed greatly to our understanding of the mechanisms underlying the development of hormone-refractory prostate cancer. This approach has clearly demonstrated the reinstatement of the AR transcriptional program as a consistent feature of AI tumors (17, 18) and the significance of AR overexpression in resistance to hormone therapy (19). Elevated expression of genes encoding PI3K/Akt/mTOR pathway components has also been implicated in androgen independence (18). Androgen-repressed genes significantly influence the transition to androgen independence as they contribute to the androgen withdrawal phenotype and to survival in the absence of androgen.

De-repression of the UDP-glucuronosyltransferase (UGT2B7/15/17) genes further suppresses AR signaling by catalyzing the inactivation and elimination of remaining 5α-dihydrotestosterone (5α-DHT) via glucuronidation (20). At the same time, resistance to androgen ablation is mediated by up-regulation of the anti-apoptotic gene clusterin (testosterone-repressed prostate message 2) (21); conversely, clusterin antisense oligodeoxynucleotides induced apoptosis of Shionogi tumors cells and delayed recurrence (21). Accordingly, the identification and targeting of anti-apoptotic genes up-regulated during androgen ablation is of substantial interest for the treatment of prostate cancer (21).

In this manuscript, we describe the identification of *CHES1* by microarray as a gene induced by androgen withdrawal in LNCaP prostate cancer cells. *CHES1* was discovered by Pati and co-workers as a forkhead/winged-helix transcription factor that complemented defective DNA damage checkpoint pathways in yeast (22). We have extended their findings to characterize the role of *CHES1* in a mammalian system. RNAi experiments demonstrated that CHES1 contributed to the basal proliferation of LNCaP and was critical to survival in the absence of androgen. In contrast, enforced expression of *CHES1* inhibited growth of LNCaP and induced the acquisition of a NE phenotype. Biochemical characterization of the LNCaP-*CHES1* subline demonstrated constitutive, nuclear localization of CHES1 and features of androgen withdrawal, such as significantly reduced AR expression and elevated serine 473-phosphorylated Akt and NSE levels.

## MATERIALS and METHODS

### Cell Lines and Culture.

LNCaP prostate adenocarcinoma cells were obtained from the American Type Culture Collection (ATCC, Manassas, VA) and maintained in RPMI 1640 medium (GIBCO BRL) supplemented with 10% fetal bovine serum (HyClone Laboratories, Logan, UT), 2 mM L-glutamine, and 100 U/ml penicillin-100 µg/ml streptomycin at 37°C in a humidified environment of 5% $CO_2$ in air. LNCaP-*CHES1* sublines were maintained in the same medium under antibiotic selection by supplementation with GENETICIN (G418 sulfate, 400 µg/ml; Invitrogen Life Technologies, Carlsbad, CA). To simulate conditions of androgen ablation, cultures were shifted into RPMI 1640 medium (without phenol red) supplemented with 10% charcoal/dextran-treated fetal bovine serum (CDT-FBS; HyClone). Androgen-independent LNCaP-cds cell lines have been described (16) and were maintained under conditions of chronic androgen deprivation in the medium described above .

### Reagents.

5$\alpha$-DHT was purchased from Sigma Chemical Company (St. Louis, MO). Wortmannin was purchased from Calbiochem (San Diego, CA). Mouse monoclonal antibodies against the androgen receptor (clone AR 441, Ab-1) and NSE (clone E27, IgG1) were purchased from Lab Vision Corporation, (Fremont, CA). Rabbit polyclonal anti-phospho(Ser473)-Akt and anti-Akt antibodies were purchased from Cell Signaling Technology (Beverly, MA). Epitope tag antibodies used in this study included mouse monoclonal anti-HA (HA.11, clone 16B12) purchased from Covance Research Products (Berkeley, CA) and anti-c-myc mouse monoclonal antibody (clone 9E10, IgG1, kappa) from Roche Applied Science (Indianapolis, IN). Rabbit polyclonal anti-phospho-FKHRL1 (Thr 32) and anti-FKHRL1 antibodies were purchased from Upstate Biotechnology, Inc. (Lake Placid, NY). The mouse monoclonal antibody against GAPDH (clone 6C5) was obtained from Chemicon International (Temecula, CA).

### Immunoblot Analysis.

NP-40 lystates were prepared from cell cultures and analyzed by immunoblot analysis according to standard protocols as previously described (23).

### Oligonucleotide Microarrays.

Human Genome U95A (HG-U95Av2) GeneChip arrays were purchased from Affymetrix (Santa Clara, CA) and provide coverage of 12,599 RNA messages. Each transcript is represented by a probe set consisting of 10 different perfect match probes (25-mers) and a corresponding set of mismatch probes. Complete design and sequence information for each probe set are available at the NetAffx website (http://www.affymetrix.com/analysis/index.affx).

### Microarray Gene Expression Profiling and Data Analysis.

GeneChip® expression analysis steps including RNA isolation, cDNA synthesis, preparation of biotin-labeled target cRNA, hybridization, washing, staining, and scanning were performed using standard protocols and reagents described by the manufacturer and as previously described (16). Scanned chip images were scaled to an average hybridization intensity of 125 with Affymetrix Microarray Suite (MAS) software algorithms. Feature extraction, data normalization, comparison analysis, and hierarchical clustering were performed using DNA-Chip Analyzer (dChip) (24). Probe set signal intensities were generated using the perfect match/mismatch model and the data was filtered to select for transcripts having a minimum normalized probe intensity value of 80 and a fold change in expression of $\geq$2.5 at the 96-hour

time point compared to that of LNCaP cells cultured in the presence of androgen. The hierarchical clustering algorithm was utilized to organize the expression data into sets of genes displaying similar expression patterns across the time course of androgen withdrawal.

**Analysis of the *CHES1* Genomic Locus.**

The exon/intron organization of the CHES1 gene was determined by BLAST analysis of the human genome using the 1,473-bp CHES1 cDNA sequence (NM_005197). The corresponding genomic contig (NT_026437.10|Hs14_26604:69517542-69830120) from chromosome 14 was downloaded and mined for androgen response elements (AREs) and regions (ARRs) using a composite of ARE/ARR consensus sequences [(A/G)(G/T)A(A/T)C(A/T/G)nnn(A/T/G)G(T/A/C)(T/A)(C/A)(T/G/C)] with GeneTool version 1.0 software (BioTools Incorporated, Edmonton, Alberta, Canada). Human genome resources were provided by the National Center for Biotechnology Information (Bethesda, MD).

**RNA Isolation and RT-PCR Analysis.**

Total RNA was isolated using the TRIzol reagent (Invitrogen, Carlsbad, CA). First-strand cDNA was prepared from 5 µg total RNA using SuperScript II reverse transcriptase (Invitrogen, Carlsbad, CA) and an oligo(dT)$_{12\text{-}18}$ primer as previously described (23). PCR reactions were performed with custom-synthesized primers (Integrated DNA Technologies, Coralville, IA). Sequences of the primers are as follows. CHES1 (CHES1 1002.For 5´-TCACAACTACAGCAGTGCCAAGTC-3´ and CHES1 1367.Rev 5´-GCTTCTTTCATCTCCTCATCATCG-3´), TUBA3 (TUBA3_100.For 5´-ATGCGTGAGTGCATCTCCATCCAC-3´ and TUBA3_624.Rev 5´-GGGCGCCGGGTAAATAGAGA-3´), GAPD (GAPD 212.For 5´-GAAATCCCATCACCATCTTCCAG-3´ and GAPD 524.Rev 5´-ATGAGTCCTTCCACGATACCAAAG-3´), AR (hAR 2756.For 5´-CCCATTGACTATTACTTTCCACCCC-3´ and hAR 3490.Rev 5´-TTGAGAGAGGTGCCTCATTCGGAC-3´), and p21$^{Cip1/Waf1}$ (p21CIP1_139.For 5´-GAGCGATGGAACTTCGACTTTG-3´ and p21CIP1_491.Rev 5'-GGCTTCCTCTTGGAGAAGATCAG-3´). PCR reactions were performed with AmpliTaq DNA polymerase (Applied Biosystems, Foster City, CA) under the following conditions: 94°C, 5 minutes; 30 cycles (94°C, 30s; 56°C[p21$^{Cip1/Waf1}$]/57°C[GAPD]/59°C[TUBA3]/60°C[CHES1, AR], 30s; 72°C, 60s); 1 cycle (72°C, 2 minutes). Amplification products were analyzed on 1.0% or 1.5% TAE-agarose gels and photographed under UV illumination.

**RNA Interference.**

Small interfering RNA duplexes (siRNAs) targeting *CHES1* were designed using standard parameters (25) and custom-synthesized (Dharmacon Research, Lafayette, CO). The location of the targeted transcript regions (*i.e.*, relative to the translation start site) and siRNA duplex sequences are as follows. The CHES1-Ri-1 siRNA targeted nucleotides 412-432; sense: 5´-GGAUAUCUACAACUGGAUCdTdT-3´, antisense: 5´-GAUCCAGUUGUAGAUAUCCdTdT-3´. CHES1-Ri-2 siRNA targeted nucleotides 421-441; sense: 5´-CAACUGGAUCUUGGAACAUdTdT-3´, antisense: 5´-AUGUUCCAAGAUCCAGUUGdTdT-3´. CHES1-Ri-3 siRNA targeted nucleotides 993-1013; sense: 5´-AGGAGGAUCACAACUACAGdTdT-3´, antisense: 5´-CUGUAGUUGUGAUCCUCCUdTdT-3´. An RNA duplex sequence targeting nucleotides 153-175 of the firefly (*Photinus pyralis*) luciferase gene in the pGL-2 Control reporter vector (accession #: X65324) was used as a control for non-specific siRNA effects (26).

For analysis of RNAi-mediated suppression of gene expression, cells were seeded into 6-well plates (2.5 x $10^5$ cells/well) and transfected in serum-containing medium (without antibiotics) with 100 nM small interfering RNA duplexes using Oligofectamine Reagent (Invitrogen, Carlsbad, CA) according to the protocol described by Harborth and co-workers (26). RNA was isolated after 48 hours of treatment for RT-PCR analysis. For cell proliferation assays, cells were seeded into 96-well plates (1 x $10^4$ cells/well) in the presence (FBS) or absence (CDT-FBS) of androgen and transfected the following day. After 72 hours, relative cell proliferation was determined using the MTS cell proliferation assay reagent (Promega, Madison, WI).

**Construction of CHES1 Mammalian Expression Plasmids.**

The full-length CHES1 coding region was generated by reverse transcription and high fidelity PCR amplification (Expand High Fidelity PCR System, Roche Applied Science, Indianapolis, IN) of total RNA prepared from LNCaP cells androgen-deprived for seven days. Gel-purified amplicons were cloned into pCR2.1-TOPO by TOPO TA cloning (Invitrogen, Carlsbad, CA) and sequence integrity confirmed by automated DNA sequencing (Davis Sequencing, Davis, CA). For expression with a twelve-amino acid hemagglutinin (HA) epitope tag (MGYPYDVPDYAS), the insert generated with CHES1_133_Cpo.For (5´-CGGTCCGATGGGTCCAGTCATGCCTCCCAG-3´) and CHES1_1605_ Xho.Rev (5´-CTCGAGTTAATTTTTTGTGGTTTCCTTTTGCTC-3´) primers was subcloned into *Cpo*I + *Xho*I-digested pcDNA3.1-CMV-HA-Neo(+)—modified from pcDNA3.1(+) (Invitrogen, Carlsbad, CA). For expression of CHES1 with a carboxyl-terminal *myc*-His epitope, the insert generated with CHES1_130 _KS.For (5´-GCCACCATGGGTCCAGTCATGCCTCCCAG-3´) and CHES1_1602_Xba.Rev (5´-TCTAGAATTTTTTGTGGTTTCCTTTTGCTC-3´) primers was subcloned into *Not*I + *Xba*I-digested pcDNA3.1(+)/*myc*-His A (Invitrogen, Carlsbad, CA).

**Establishment of LNCaP Sublines Stably Expressing CHES1.**

LNCaP cells were transfected with pcDNA3.1-CMV-HA-*CHES1* or pcDNA3.1(+)-*CHES1*-*myc*-His expression constructs using Effectene transfection reagent (Qiagen, Valencia, CA) according to the manufacturer's protocol. Stably-transfected clones and pools were selected by culture in the presence of GENETICIN antibiotic (400 µg/ml).

## RESULTS

### LNCaP Cells Subjected to Androgen Withdrawal Exhibit Features Typical of Androgen Ablation.

In order to better understand the mechanisms responsible for the survival of prostate cancer cells during androgen ablation, we simulated this modality *in vitro* using the LNCaP human androgen-dependent prostate cancer cell line subjected to androgen deprivation as a model system. Levels of expression or activation of selected proteins associated with AR signaling were evaluated by immunoblot analysis of NP-40 lysates prepared from cells harvested one to forty-five days after androgen withdrawal. As shown in **Figure 1A**, androgen deprivation triggered a rapid and marked reduction in AR protein levels and a corresponding decrease in the expression and secretion of prostate-specific antigen (PSA) (23). Although this treatment does not induce apoptosis (*data not shown*), it induces growth arrest and transdifferentiation of LNCaP cells into a neuroendocrine (NE) phenotype (2). This was verified by biochemical and morphological criteria, such as increased NSE expression **(Fig. 1A),** rounding of the cell bodies, and extension of neuritic processes **(Fig. 1B)**. A marked and persistent increase in the levels of activated Ser473-phosphorylated Akt/PKB was also observed **(Fig. 1A)**. In summary, androgen deprivation promotes the appearance of classic features of androgen ablation triggered by attenuated AR pathway signaling resulting in NED, growth arrest, and PI3K/Akt pathway hyperactivation supporting survival of this PTEN-deficient model (3).

### Identification of *Checkpoint Suppressor 1* (*CHES1*) as an Androgen Withdrawal-induced Gene by Expression Profiling of LNCaP Cells.

Microarray gene expression profiling was utilized to identify androgen-regulated genes that might support survival and mediate the appearance of one or more features accompanying androgen ablation. RNA was isolated from cells either left untreated in the presence of 1 nM DHT or deprived of androgen for 0.5, 6, 24, and 96 hours followed by analysis of approximately 12,599 transcripts using Affymetrix HG-U95Av2 GeneChip oligonucleotide arrays. Differentially expressed genes and groups, or clusters, of genes displaying similar expression patterns were identified by comparison analysis and hierarchical clustering (24). Since we hypothesized that the genes most likely to impact upon cell physiology during chronic androgen deprivation would be those exhibiting the greatest and persistent changes, our analysis was focused to select only those genes that were differentially expressed by at least $\geq$2.5-fold at the 96-hour time point. This yielded a set of 159 genes divided into two major clusters of 78 up-regulated and 81 down-regulated genes exhibiting changes ranging from 2.72- to 134.53-fold and –2.69- to -68.24-fold, respectively **(Supplementary Tables 1 and 2, Fig. 2A)**. The efficacy of androgen deprivation in this experiment was validated by *1)* the attenuation of androgen-induced gene expression, such as PSA, kallikrein 2, NKX3.1, and TCR gamma alternate reading frame protein and by *2)* the induction of typically androgen-repressed genes including $\alpha$3-tubulin, insulin-like growth factor binding protein 3, UGT2B17 (20), and clusterin (27, 28) **(Fig. 2B)**.

In these experiments, *checkpoint suppressor 1* (*CHES1*; FOXN3) was identified as an androgen withdrawal-induced gene, exhibiting 2.65- and 3.25-fold induction of expression following 24 and 96 hours of androgen deprivation, respectively **(Supplementary Table 1, Fig. 2A)**. Compared to several other androgen-regulated genes, the magnitude and kinetics of expression was most similar to that displayed by clusterin **(Fig. 2B)**. RT-PCR analysis validated these findings **(Fig. 2C)** and also demonstrated that *CHES1* was expressed at very low levels in androgen-independent LNCaP-cds cell lines derived by selection under long-term androgen-deprivation (16). These data demonstrate that *CHES1* expression is up-regulated in androgen-dependent

LNCaP cells during acute androgen withdrawal, but returns to basal levels after reinstatement of the AR pathway in androgen-independent sublines.

We pursued the role of *CHES1* in CaP biology for several reasons. In addition to its prominent expression in response to androgen deprivation, CHES1 might serve a pivotal function in mediating androgen withdrawal-induced growth arrest and survival; It was originally identified by virtue of its ability to reinstate a G2/M DNA damage checkpoint in several mutant yeast strains, thereby suppressing the lethality of those checkpoint defects (22). Additionally, *CHES1* is a member of the forkhead/winged-helix family, suggesting it has the capacity to influence one or more pathways via its transcriptional targets.

**_CHES1_ Expression Is Potentially Suppressed by p53 Activation.**

Since *CHES1* complemented multiple DNA damage checkpoint pathway defects in yeast (22), we hypothesized that CHES1 might function as an effector molecule in a pathway unique to mammalian cells, namely the p53 pathway. To investigate this, *CHES1* expression was analyzed in LNCaP cells exposed to ionizing radiation (IR). As shown in **Fig. 2D**, $\gamma$-irradiation (10 Gy) was successful in mediating p53 activation, as $p21^{Cip1/Waf1}$ expression was rapidly induced by two hours and peaked at four hours. In contrast, the low, basal expression of CHES1 was further down-regulated. In summary, the data suggest that *CHES1* is a primary or secondary p53 target gene.

**Structure of the _CHES1_ Genomic Locus**

To gain insight into sequence determinants responsible for the androgen-regulated expression of *CHES1*, we interrogated the genomic locus for the presence of AREs. *CHES1* resides on chromosome 14q24.3-q31 (NCBI, (22)). A genomic BLAST using the 1,473-bp *CHES1* cDNA sequence revealed that it is encoded by six exons spanning approximately 250 kbp **(Fig. 3A)**. During the cloning of the full-length *CHES1* cDNA sequence from LNCaP RNA, we independently identified *CHES1*$\beta$, an isoform of *CHES1* that lacks exon 4 and was presumably generated by alternative splicing **(Fig. 3A)**. The mouse ortholog of *CHES1*, *Mus musculus Ches1*, is located on chromosome 12 and encodes a transcript similar to the *CHES1*$\beta$ isoform. While a full-length transcript similar to *CHES1*$\alpha$ is encoded by *Mm similar to CHES1* on chromosome X, it is now classified as a pseudogene.

The 312-kbp contig containing the *CHES1* gene, including 31.2 kbp of the 5´- and 3´-untranslated regions, was scanned for consensus AR DNA binding sites using a consensus ARE motif derived from a composite of published sequences (29, 30). This revealed thirty-three potential AREs **(Fig. 3B)**. Although the presence of androgen strongly represses *CHES1* expression, we did not identify any sites in the proximal promoter or enhancer regions of the gene. However, intron 3 contained seventeen AREs, most of which (13/17) are concentrated to its distal region. In summary, transcriptional repression of *CHES1* by androgen is potentially mediated by the binding of the AR to sequence motifs in intron 3 rather than to *cis*-regualtory elements in the 5´-untranslated region of the gene.

**RNAi-mediated Silencing of _CHES1_ Expression Induces Growth Inhibition and Apoptosis in the Absence of Androgen.**

In order to determine the potential contribution of CHES1 to the maintenance of LNCaP cell growth and viability, the effects of CHES1 silencing were evaluated. For this, cells were transfected with siRNA duplexes, cultured in the presence or absence of androgen for three days, and relative proliferation rates were determined by MTS assays. Treatment with each of the CHES1 siRNAs resulted in growth inhibition **(Fig. 4A)**. In the presence of androgen, this ranged from 27-38% when compared to the growth of cultures treated with a control siRNA

targeting luciferase. In the absence of androgen, inhibition reached 45% with the CHES1-Ri-1 siRNA. Light microscopic examination revealed that apoptosis was induced by this duplex specifically in the absence of androgen as evidenced by the appearance of distinctive features, such as cellular fragmentation and condensation of cytoplasmic contents **(Fig. 4B,** *compare CHES1-Ri-1 panels, -DHT and +DHT***)**. The efficacy and specificity of the CHES1-Ri-1 was demonstrated by its ability to reduce *CHES1* expression by approximately 70% and by the absence of effects upon a non-targeted gene (*e.g.*, AR), respectively **(Fig. 4C)**.

**CHES1 Is Expressed as a 56-kD Protein Localized Primarily in the Nucleus.**

LNCaP sublines stably expressing CHES1 were established in order to study the effects of its enforced expression in this CaP model. The full-length *CHES1* cDNA was cloned and expressed as an amino-terminal HA- or carboxyl-terminal *mycHis* epitope-tagged protein. Since CHES1 is a transcription factor, its cellular localization was of particular interest; therefore, as an initial step in its biochemical characterization, nuclear and cytosolic fractions of LNCaP-*HA-CHES1* and LNCaP-*CHES1-mycHis* cells were immunoblotted for CHES1 expression. In both cases, CHES1 migrated with an apparent molecular mass of ~56 kD and its expression was predominantly nuclear **(Fig. 5A)**. This contrasted its family member FKHRL1, which exhibits phosphorylation-regulated localization, being primarily cytosolic in the presence of PI3K/Akt pathway activation, but rapidly shifting to the nucleus upon its dephosphorylation during PI3K inhibition with wortmannin **(Fig. 5B)**.

**Enforced Expression of CHES1 in LNCaP Cells Induces Phenotypic and Biochemical Features Characteristic of Androgen Withdrawal.**

Next, the influence of CHES1 upon LNCaP biology was evaluated. Enforced CHES1 expression resulted in morphological changes indicative of NED characterized by rounded cell bodies and the extension of short neuritic processes, similar to that observed for LNCaP-*vector* cells subjected to androgen withdrawal **(Fig. 6A**, *compare LNCaP-CHES1 panels to LNCaP-vector in CDT-FBS***)**. In contrast to LNCaP-*vector* cells, the NE phenotype of LNCaP-*CHES1* cells did not require androgen deprivation and was evident even in the presence of androgen (*see FBS and CDT-FBS+DHT panels*). Constitutive expression of CHES1 in LNCaP also resulted in a significant decrease in proliferation in the presence of androgen, as LNCaP-*CHES1* cultures exhibited total cell numbers 42% less than that of LNCaP-*vector* cells after five days **(Fig. 6B)**. In the absence of androgen, both cell lines displayed markedly attenuated growth. Having observed that stable CHES1 expression induced growth inhibition and NE differentiation, we wanted to determine if it imparted biochemical features of androgen deprivation. To that end, the levels of selected proteins characteristic of androgen ablation **(Fig. 1A)** were compared in LNCaP-*CHES1* cells and in LNCaP-*vector* cells subjected to androgen withdrawal for three and five days. As shown in **Figure 6C**, LNCaP-*CHES1* possessed a very similar profile to that of androgen-deprived LNCaP cells. AR levels were markedly down-regulated, and only detectable upon longer exposures (*data not shown*). NSE expression was significantly increased, consistent with the NE phenotype of LNCaP-*CHES1*. In addition, serine473-phosphoryated Akt and total Akt levels were greatly elevated. Taken together, these data demonstrate that stable expression of CHES1 can recapitulate several events triggered by androgen ablation.

## DISCUSSION

The primary goal of these experiments was to identify and characterize novel androgen withdrawal-regulated genes as they are potentially critical in mediating the biological effects of this treatment and in antagonizing apoptosis. The results of our microarray analysis of LNCaP cells subjected to androgen deprivation generated a transcriptional program composed of 159 differentially expressed genes (*i.e.*, $\geq$2.5-fold) signifying the occurrence of androgen ablation and NED. Although the design of our study was opposite to that of previously described studies involving stimulation with androgen (29, 31), it yielded consistent results in terms of the number (*i.e.*, 146 genes displaying $\geq$3.0-fold changes) (29) and identities of androgen-responsive genes **(Supplementary Tables 1 and 2; Fig. 2, A and B)**. In addition, elevated expression of CD24 antigen and $\alpha$-tubulin (TUBA3) was in accord with NED and similar to that observed in LuCaP 49 prostatic small-cell, NE carcinoma xenografts (32).

*CHES1* displayed an expression pattern typical of an androgen-repressed gene **(Supplementary Tables 1 and 2; Fig. 2, A and B)**. Although we do not have experimental evidence, the results of *in silico* analysis of the *CHES1* genomic locus suggest that it would not be controlled by AR binding to the proximal promoter region or even an upstream enhancer in the 5´-UTR since the nearest putative ARE is located at position -27,386 (*i.e.*, relative to the start site). In contrast, 27 putative ARE/ARR's were found in introns 1, 2, 3, and 5 **(Fig. 3B)**. Similarly, AREs contained in enhancer elements responsible for the tissue-specific expression and androgen repression of the prostate-specific membrane antigen/folate hydrolase 1 (33) and AR (34) genes have not been found in their promoters or 5´-flanking regions, but rather reside in the third intron 12-kbp downstream from the start site or in exons 4/5, respectively. Whether or not *CHES1* is a direct or secondary AR target gene remains to be determined.

*CHES1/FOXN3* represented an exciting androgen withdrawal-induced gene since it had been discovered as a putative human checkpoint gene by virtue of its ability to suppress the lethality of multiple checkpoint-deficient yeast strains caused by genotoxic stresses, such as ultraviolet and ionizing radiation and methyl methanesulfonate (22). The full-length *CHES1* transcript encodes a forkhead/winged-helix transcription factor most similar to the FOXN subfamily members WHN/FOXN1 and HTLF/FOXN2 (22). Its predicted molecular mass of 54-kD for the 491-amino acid open reading frame was confirmed in this study **(Fig. 5A)**. However, the ability to increase survival is attributed to its capacity to restore the DNA damage-induced delay of G2/M progression through directly interacting with the corepressor Sin3 and consequently inhibiting the Sin3/Rpd3 HDAC complex (35). HDAC can participate in the recognition of damaged DNA through the formation of a complex with Rad9 (36). Taken together, this suggests that in addition to global effects upon gene transcription, modulation of HDAC activity by CHES1 could also regulate the accessibility of damaged DNA to Rad repair complexes.

The results of our experiments suggest that *CHES1* contributes to the regulation of cell growth and apoptosis of human prostate cancer cells. RNAi-mediated silencing of *CHES1* expression caused a moderate reduction in both the basal androgen-dependent growth of LNCaP cells as well as growth in androgen-deprived medium **(Fig. 4A)**. It is worth noting that the magnitude of this effect might be underestimated since the siRNA transfection efficiency was approximately 80%. Our findings are in accord with previous reports that demonstrated forkhead transcription factors in humans (FKHRL1) (37) and yeast (*Fkh1*, *Fkh2*) (38) promoted cell cycle progression via their action on G2/M promoters, such as *cyclin B* and *polo-like kinase*. The anti-apoptotic role for CHES1 during androgen withdrawal was brought to light by the ability of CHES1 siRNAs to convert combined growth inhibition and NED to an apoptotic response **(Fig. 4B)**. This is consistent with its previously described survival properties in response to genotoxic insults (22) as well as its ability to functionally replace *MEC1* (yeast homolog of

ATM/ATR) as an essential factor for growth of yeast even in the absence of DNA damage. Additionally, RNAi of *CHES1-like* induced marked apoptosis of *Drosophila melanogaster* macrophage-like S2 cells (39). Due to the toxicity of *CHES1* silencing during androgen withdrawal, these experiments were inconclusive in terms of defining a role for *CHES1* in NED. We observed that *CHES1* expression was repressed in response to p53 activation by IR **(Fig. 2D)**. This might be explained by the presence of a putative p53 half-site in the *CHES1* promoter (*data not shown*). Although it was not cytotoxic, IR has been reported to sensitize LNCaP cells to TRAIL-mediated apoptosis through the coordinated up-regulation of death receptor 5 and modulators of the intrinsic apoptosis pathway, Bax, and Bak (40). Similarly, the anti-cancer agents mitomycin C and doxorubicin were shown to increase apoptosis susceptibility via a p53-dependent induction of the CD95/APO-1/Fas death receptor (41) and cytotoxic doses of both of these agents repressed the expression of *CHES1* in HepG2 human hepatocellular carcinoma cells (42). Consistent with p53-mediated *CHES1* repression as a pro-apoptotic mechanism, it is noteworthy that long-term androgen withdrawal was accompanied by diminished p53 protein levels (*data not shown*).

The growth rate of LNCaP-*CHES1* was retarded by approximately 42% compared to that of vector-transfected cells **(Fig. 6B)**. While this result was paradoxical when considered together with the findings from our RNAi experiments **(Fig. 4A)**, it might be explained by the fact that enforced expression of *CHES1* at elevated levels mediated a cellular response of differentiation (*discussed below*) and growth inhibition. In the LNCaP model, there are precedents for one stimulus mediating opposite responses. While androgen is a potent mitogen at physiological concentrations, growth repression and apoptosis occur at supraphysiological doses (43). In fact, AI LNCaP sublines established by long-term cultivation in hormone-depleted medium consistently exhibit a paradoxical growth inhibition in response to androgenic stimulation (16, 44). Along the same line, Akt-mediated phosphorylation of the AR has differential effects on its activity in that it can suppress AR activity at low passage numbers or enhance it at higher ones (45).

Stable expression of *CHES1* in LNCaP partially recapitulated the biological and molecular responses to androgen withdrawal. The acquisition of a NE phenotype of LNCaP-*CHES1* cells was evidenced both morphologically and biochemically **(Fig. 6, A and C)** and was very stable in that it was not altered by hormonal manipulation **(Fig. 6A)** and has remained unchanged to date. The ability of *CHES1*/*FOXN3* to induce differentiation was not completely unexpected as *Whn*/*FOXN1*, whose mutation gives rise to the *nude* phenotype in mice and rats, has an obligatory function in terminal differentiation of cutaneous and thymic epithelial cells (46). Since *CHES1* overexpression did not induce NED identical in appearance to that of androgen withdrawal, we interpret this to indicate that it acts in concert with other components of the differentiation program and potentially at a later stage, based upon the kinetics of its expression. As an example, increased expression of receptor-type protein-tyrosine phosphatase alpha during androgen deprivation has also been implicated as a vital component of NED via MAPK/ERK signaling (47). Interestingly, the NED phenotype in LNCaP varies with the stimulus, such as interleukin-6 (48) and agents which elevate intracellular cAMP levels and activate protein kinase A (49). It was surprising that *CHES1* could promote NED in the presence of androgen, but the markedly diminished levels of AR in LNCaP-*CHES1* cells **(Fig. 6C)** could explain this since it has been reported that silencing of *AR* expression was sufficient to induce NED (8). While markedly elevated Akt activation **(Fig. 6C)** was an additional characteristic of androgen withdrawal, it also poses as a mediator of AR protein diminution via triggering ubiquitin-mediated degradation by its phosphorylation of the AR (50). Interestingly, it has recently been reported that Whn/FOXN1 induced the expression of Akt and chromogranin A during terminal differentiation of primary human keratinocytes (46).

The identification and role of human *CHES1* as a critical mediator of G2/M and mitotic spindle checkpoints, basal cell growth, and enhancement of survival in response to genotoxic stresses have been elegantly elucidated in the yeast system (22, 35). In this manuscript, we extended these findings to characterize its role in prostate cancer biology. Our results demonstrated that it is regulated in an androgen- and p53-repressed manner and was capable of recapitulating phenotypic and molecular features of androgen withdrawal. CHES1 also contributes to the androgen-dependent growth of LNCaP cells and confers resistance to apoptosis during androgen withdrawal. Since *CHES1* silencing resulted in apoptosis specifically during androgen ablation, the adjuvant use of agents that antagonize its expression or function might be effective in delaying the development of hormone refractory disease.

**ACKNOWLEDGEMENTS**

The authors wish to thank Dawn B. Milliken and Ryan R. Davis (Department of Pathology and Laboratory Medicine, UC Davis School of Medicine) and Robert Wang (Mira Loma High School, Sacramento, CA) for expert technical assistance and valuable discussion. We are grateful to Dr. Xu-Bao Shi (Department of Urology, University of California, Davis School of Medicine) for generously providing the LNCaP-cds cell lines and to Dr. Susan L. Scott for assistance with the radiation studies. We also wish to thank Dr. Dan R. Robinson (UC Davis Cancer Center) for the gift of the pcDNA3.1-CMV-HA expression vector.

## ABBREVIATIONS

AI, androgen-independent; AD, androgen-depleted; AR, androgen receptor; ARE, androgen response element; ARR, androgen response region; AW, androgen withdrawal; CaP, carcinoma of the prostate; CDT-FBS, charcoal/dextran-treated-FBS; *CHES1*, checkpoint suppressor 1; DBD, DNA binding domain; FBS, fetal bovine serum; GAPD, glyceraldehyde 3-dehydrogenase; HDAC, histone deacetylase; IGF-1, insulin-like growth factor-1; IR, ionizing radiation; NE, neuroendocrine; NED, neuroendocrine differentiation; NSE, neuron-specific enolase; PI3K, phosphatidylinositol 3-kinase; PSA, prostate-specific antigen; RNAi, RNA interference; SAGE, serial analysis of gene expression; siRNA, small interfering RNA.

## FIGURE LEGENDS

**Figure 1. Androgen ablation of LNCaP induces marked modulation of AR-regulated protein levels and neuroendocrine differentiation.** ***(A)*** LNCaP cells were left untreated in the presence of DHT (1 nM) or were subjected to conditions of androgen ablation for a duration of 1-45 days by culturing in RPMI 1640 medium (without phenol red) supplemented with CDT-FBS. Immunoblot analysis of NP-40 lysates was performed for the determination of AR, NSE, phospho(Ser473)-Akt, and total Akt levels. Migration of molecular weight standards is indicated. ***(B)*** Morphology of LNCaP cells cultured for five days in the presence or absence of androgen was evaluated by phase contrast microscopy at 200X magnification. Androgen withdrawal induced the appearance of characteristics typical of NED, such as extension of neuritic processes and rounded cell bodies.

**Figure 2. Microarray analysis of LNCaP cells subjected to androgen withdrawal yields a distinctive expression profile characterized by marked up-regulation of *CHES1*.** ***(A)*** Total RNA was prepared from LNCaP cells cultured in the presence of androgen (+*DHT*) and subjected to androgen withdrawal (-*DHT*) for 0.5, 6, 24, and 96 hours. Global gene expression profiling was performed with Affymetrix HG-U95Av2 GeneChip oligonucleotide arrays as described in *Materials and Methods*. Comparison analysis and hierarchical clustering (dChip) were used to identify transcripts that exhibited $\geq$2.5-fold differential expression at the 96-hr time point and then to group those with similar expression patterns, respectively. The resulting cluster diagram depicts two major clusters of *androgen withdrawal (AW)-repressed* and *AW-induced* genes. The mean expression value for each gene throughout the time course was determined and the magnitude of increased or decreased expression at each time point relative to the mean is depicted by increasingly darker shades of red or blue, respectively. As shown in the right panel, *CHES1* segregated with the "AW-induced" gene cluster containing 78 transcripts and displayed strong induction by 24 hours. ***(B)*** *CHES1* is up-regulated during androgen withdrawal and exhibits kinetics comparable to other "androgen-repressed" genes. Fold changes in expression (relative to LNCaP cultured in the presence of androgen; +*DHT*, *empty bars*) for *CHES1* and the indicated androgen-regulated genes at each time point were determined by comparison analysis of the data obtained from the microarray experiment described in ***Fig. 2A***. Results are graphically represented for each gene following 0.5 (*diagonally-hatched bars*), 6 (*horizontally-lined bars*), 24 (*checkered bars*), and 96 (*solid bars*) of androgen withdrawal. ***(C)*** AW-induced CHES1 expression was validated by standard RT-PCR analysis of total RNA prepared from LNCaP cells at the indicated times after the beginning of androgen deprivation. Expression in androgen-independent LNCaP-cds cell lines (clones 1 and 2) was also evaluated. $\alpha$3-tubulin levels were monitored as a positive control for AW-induced gene expression and glyceraldehyde 3-phosphate dehydrogenase (GAPD) as a loading control and for normalization. ***(D)*** *CHES1* expression is suppressed by p53 activation. LNCaP cells

($2.5 \times 10^6$) were seeded in 10-cm dishes and subjected to ionizing radiation (10 Gy) for the indicated times or left untreated for 24 hours (*Con*). Total RNA was isolated and analyzed by RT-PCR for the expression of CHES1, $p21^{Cip1/Waf1}$, and β-actin.

**Figure 3. *CHES1* genomic locus and mapping of potential androgen-response elements.** ***(A)*** Structure of the *CHES1* gene and polypeptide. The *CHES1* genomic locus maps to chromosome 14q24.3-q31 (22) and encodes six exons. These were identified by BLAST analysis of human genome sequence (NCBI) with the full-length 1,473-bp *CHES1* cDNA sequence (NM_005197[gi:4885136]) and are shown positioned along contig NT_026437.10 containing the CHES1 locus. The full-length isoform is referred to as CHES1α and encodes a 490-amino acid polypeptide. CHES1β, an alternatively spliced variant lacking exon 4, is also present in LNCaP. The structures of the mouse (*Mus musculus*) orthologs, *Mm CHES1* and *Mm similar to CHES1*, are shown for comparison. The conserved forkhead/winged helix domain is shaded in gray. ***(B)*** Putative sites of AR binding in the *CHES1* gene. The 312.6-kbp contig sequence containing the entire *CHES1* coding region and 5´- and 3´- untranslated regions was screened for the presence of AREs and ARRs and are depicted as hash marks. The consensus sequence used for screening is shown below the schematic.

**Figure 4. RNAi-mediated CHES1 silencing induces growth inhibition and apoptosis of LNCaP cells.** ***(A)*** LNCaP cells were seeded in 96-well plates ($1 \times 10^4$ cells/well) in the presence (+*DHT*) or absence (-*DHT*) of androgen and transfected with one of three CHES1-specific siRNA duplexes (100 nM) as described in *Materials and Methods*. As a control for any non-specific effects of the transfection reagent and/or siRNA duplex, cells were also transfected with an siRNA that targeted the firefly luciferase gene. Following a three-day incubation, proliferation was determined by MTS assay. The mean absorbance (A490 nm) of quadruplicate wells for each CHES1 siRNA-treated group was used to determine fractional growth relative to the control siRNA treated group (*empty bars*). Results are expressed as percentage growth inhibition for each CHES1 siRNA (*diagonally-hatched, checkered, and solid bars*) relative to the control ± S.D. ***(B)*** LNCaP cells were seeded in 6-well plates under the growth conditions described in *panel A* and transfected with CHES1 (*CHES1-Ri-1*) or luciferase (*Control*) siRNAs. Cell morphology was examined by phase contrast microscopy under 200x magnification. In the absence of androgen (-*DHT*), CHES1 RNAi induced characteristic features of apoptosis. ***(C)*** Total RNA was isolated from samples treated identically as in *panel B* as well as from cells mock-transfected with siRNA universal buffer (*UB*). RT-PCR analysis of CHES1 and AR expression was performed and validated the effectiveness and specificity of the CHES1 siRNA (*Ri*) treatment.

**Figure 5. CHES1 is constitutively localized to the nucleus.** ***(A)*** Nuclear and cytosolic extracts were prepared from LNCaP sublines stably transfected with *myc*His or HA epitope-tagged CHES1 expression constructs and subjected to immunoblot analysis to examine CHES1 cellular localization. LNCaP cells transfected with empty vector (*Vector*) were included as a negative control. Tagged CHES1 was detected by probing with monoclonal anti-HA (*upper panel*) or anti-*myc* (*lower panel*) antibodies. CHES1 expression was detected primarily in the nuclear fraction. Migration of molecular weight standards are indicated on the left-hand side of the gel. The anti-*myc* antibody also detected a non-specific protein migrating at ~49.8 kD. ***(B)*** Phosphorylation-regulated FKHRL1/FOXO3A cellular localization was demonstrated by immunoblot analysis of nuclear and cytosolic extracts from LNCaP cells treated with the PI3K inhibitor wortmannin (100 nM) for 1 and 3 hours. The blot was developed with polyclonal anti-phospho (Thr32)-FKHRL1 and anti-FKHRL1 antibodies.

**Figure 6. Enforced expression of CHES1 recapitulates phenotypic and molecular responses of androgen withdrawal.** ***(A)*** LNCaP-*CHES1* cells have a neuroendocrine morphology. LNCaP-*CHES1* and LNCaP-*vector* cell lines were cultured in 10-cm dishes for 5

days in medium containing the indicated serum and/or androgen supplements. Digital images were acquired using phase contrast microscopy at 200x magnification. Under all conditions, LNCaP-*CHES1* cells have rounded cell bodies and neuritic processes. ***(B)*** Enforced CHES1 expression retards androgen-stimulated proliferation. LNCaP-*vector* (■, □) and LNCaP-*CHES1* (●, ○) cells were seeded in 10-cm dishes at a density of 3 x $10^5$ cells/dish. After attachment, the medium was changed to assess growth in the presence (*filled symbols*) or absence (*open symbols*) of DHT (1 nM). Cell numbers were determined for each sample in triplicate by cell counts with a Neubauer hemocytometer on days 2, 3, and 4. Results are expressed as mean total number of cells per dish ± S.D. ***(C)*** LNCaP-*CHES1* cells display biochemical features typical of LNCaP cells subjected to androgen withdrawal. NP-40 lysates were prepared from LNCaP-*vector* cells cultured in androgen-containing (*FBS*) or depleted (*CDT-FBS*) medium and from LNCaP-*CHES1* cells cultured in the presence of androgen. Immunoblot analysis was performed to confirm HA-CHES1 expression and to compare levels of AR, phospho(Ser473)-Akt, total Akt, and NSE. GAPDH was used as a loading control and molecular weight markers are indicated.

## REFERENCES


1. Turkes, A. O. and Griffiths, K. Endocrine treatment of prostate cancer. Prog Med Chem, *26:* 299-321, 1989.
2. Burchardt, T., Burchardt, M., Chen, M. W.*, et al.* Transdifferentiation of prostate cancer cells to a neuroendocrine cell phenotype in vitro and in vivo. J.Urol., *162:* 1800-1805, 1999.
3. Murillo, H., Huang, H., Schmidt, L. J., Smith, D. I., and Tindall, D. J. Role of PI3K signaling in survival and progression of LNCaP prostate cancer cells to the androgen refractory state. Endocrinology, *142:* 4795-4805, 2001.
4. Agus, D. B., Cordon-Cardo, C., Fox, W.*, et al.* Prostate cancer cell cycle regulators: response to androgen withdrawal and development of androgen independence. J Natl Cancer Inst, *91:* 1869-1876, 1999.
5. Kemppainen, J. A., Lane, M. V., Sar, M., and Wilson, E. M. Androgen receptor phosphorylation, turnover, nuclear transport, and transcriptional activation. Specificity for steroids and antihormones. J Biol Chem, *267:* 968-974, 1992.
6. Sheflin, L., Keegan, B., Zhang, W., and Spaulding, S. W. Inhibiting proteasomes in human HepG2 and LNCaP cells increases endogenous androgen receptor levels. Biochem Biophys Res Commun, *276:* 144-150, 2000.
7. Knudsen, K. E., Arden, K. C., and Cavenee, W. K. Multiple G1 regulatory elements control the androgen-dependent proliferation of prostatic carcinoma cells. J Biol Chem, *273:* 20213-20222, 1998.
8. Wright, M. E., Tsai, M. J., and Aebersold, R. Androgen receptor represses the neuroendocrine transdifferentiation process in prostate cancer cells. Mol Endocrinol, *17:* 1726-1737, 2003.
9. Hansson, J. and Abrahamsson, P. A. Neuroendocrine pathogenesis in adenocarcinoma of the prostate. Ann Oncol, *12 Suppl 2:* S145-152, 2001.
10. Desai, S. J., Tepper, C. G., and Kung, H. J. Neuroendocrine differentiation and androgen independence in prostate cancer. *In:* C. Chang (ed.), Hormone therapy of prostate cancer, Vol. In press, pp. 157-190, 2004.
11. Lin, J., Adam, R. M., Santiestevan, E., and Freeman, M. R. The phosphatidylinositol 3'-kinase pathway is a dominant growth factor-activated cell survival pathway in LNCaP human prostate carcinoma cells. Cancer Res, *59:* 2891-2897, 1999.
12. Majumder, P. K., Febbo, P. G., Bikoff, R.*, et al.* mTOR inhibition reverses Akt-dependent prostate intraepithelial neoplasia through regulation of apoptotic and HIF-1-dependent pathways. Nat Med, *10:* 594-601, 2004.
13. Catz, S. D. and Johnson, J. L. Transcriptional regulation of bcl-2 by nuclear factor kappa B and its significance in prostate cancer. Oncogene, *20:* 7342-7351, 2001.
14. Huang, H., Cheville, J. C., Pan, Y., Roche, P. C., Schmidt, L. J., and Tindall, D. J. PTEN induces chemosensitivity in PTEN-mutated prostate cancer cells by suppression of Bcl-2 expression. J Biol Chem, *276:* 38830-38836, 2001.
15. Tso, C. L., McBride, W. H., Sun, J.*, et al.* Androgen deprivation induces selective outgrowth of aggressive hormone-refractory prostate cancer clones expressing distinct cellular and molecular properties not present in parental androgen-dependent cancer cells. Cancer J, *6:* 220-233, 2000.
16. Shi, X. B., Ma, A. H., Tepper, C. G.*, et al.* Molecular alterations associated with LNCaP cell progression to androgen independence. Prostate, *60:* 257-271, 2004.

17. Amler, L. C., Agus, D. B., LeDuc, C.*, et al.* Dysregulated expression of androgen-responsive and nonresponsive genes in the androgen-independent prostate cancer xenograft model CWR22-R1. Cancer Res, *60:* 6134-6141, 2000.
18. Mousses, S., Wagner, U., Chen, Y.*, et al.* Failure of hormone therapy in prostate cancer involves systematic restoration of androgen responsive genes and activation of rapamycin sensitive signaling. Oncogene, *20:* 6718-6723, 2001.
19. Chen, C. D., Welsbie, D. S., Tran, C.*, et al.* Molecular determinants of resistance to antiandrogen therapy. Nat Med, *10:* 33-39, 2004.
20. Guillemette, C., Hum, D. W., and Belanger, A. Regulation of steroid glucuronosyltransferase activities and transcripts by androgen in the human prostatic cancer LNCaP cell line. Endocrinology, *137:* 2872-2879, 1996.
21. Gleave, M. E., Zellweger, T., Chi, K.*, et al.* Targeting anti-apoptotic genes upregulated by androgen withdrawal using antisense oligonucleotides to enhance androgen- and chemo-sensitivity in prostate cancer. Invest New Drugs, *20:* 145-158, 2002.
22. Pati, D., Keller, C., Groudine, M., and Plon, S. E. Reconstitution of a MEC1-independent checkpoint in yeast by expression of a novel human fork head cDNA. Mol Cell Biol, *17:* 3037-3046, 1997.
23. Tepper, C. G., Boucher, D. L., Ryan, P. E.*, et al.* Characterization of a novel androgen receptor mutation in a relapsed CWR22 prostate cancer xenograft and cell line. Cancer Res, *62:* 6606-6614, 2002.
24. Li, C. and Wong, W. H. Model-based analysis of oligonucleotide arrays: expression index computation and outlier detection. Proc Natl Acad Sci U S A, *98:* 31-36, 2001.
25. Elbashir, S. M., Lendeckel, W., and Tuschl, T. RNA interference is mediated by 21- and 22-nucleotide RNAs. Genes Dev, *15:* 188-200, 2001.
26. Harborth, J., Elbashir, S. M., Bechert, K., Tuschl, T., and Weber, K. Identification of essential genes in cultured mammalian cells using small interfering RNAs. J Cell Sci, *114:* 4557-4565, 2001.
27. Gregory, C. W., Hamil, K. G., Kim, D.*, et al.* Androgen receptor expression in androgen-independent prostate cancer is associated with increased expression of androgen-regulated genes. Cancer Res, *58:* 5718-5724, 1998.
28. Bettuzzi, S., Hiipakka, R. A., Gilna, P., and Liao, S. T. Identification of an androgen-repressed mRNA in rat ventral prostate as coding for sulphated glycoprotein 2 by cDNA cloning and sequence analysis. Biochem J, *257:* 293-296, 1989.
29. Nelson, P. S., Clegg, N., Arnold, H.*, et al.* The program of androgen-responsive genes in neoplastic prostate epithelium. Proc Natl Acad Sci U S A, *99:* 11890-11895, 2002.
30. Cleutjens, K. B., van Eekelen, C. C., van der Korput, H. A., Brinkmann, A. O., and Trapman, J. Two androgen response regions cooperate in steroid hormone regulated activity of the prostate-specific antigen promoter. J.Biol.Chem., *271:* 6379-6388, 1996.
31. Xu, L. L., Su, Y. P., Labiche, R.*, et al.* Quantitative expression profile of androgen-regulated genes in prostate cancer cells and identification of prostate-specific genes. Int J Cancer, *92:* 322-328, 2001.
32. Clegg, N., Ferguson, C., True, L. D.*, et al.* Molecular characterization of prostatic small-cell neuroendocrine carcinoma. Prostate, *55:* 55-64, 2003.
33. Noss, K. R., Wolfe, S. A., and Grimes, S. R. Upregulation of prostate specific membrane antigen/folate hydrolase transcription by an enhancer. Gene, *285:* 247-256, 2002.
34. Dai, J. L. and Burnstein, K. L. Two androgen response elements in the androgen receptor coding region are required for cell-specific up-regulation of receptor messenger RNA. Mol Endocrinol, *10:* 1582-1594, 1996.

35. Scott, K. L. and Plon, S. E. Loss of Sin3/Rpd3 histone deacetylase restores the DNA damage response in checkpoint-deficient strains of Saccharomyces cerevisiae. Mol Cell Biol, *23:* 4522-4531, 2003.
36. Cai, R. L., Yan-Neale, Y., Cueto, M. A., Xu, H., and Cohen, D. HDAC1, a histone deacetylase, forms a complex with Hus1 and Rad9, two G2/M checkpoint Rad proteins. J Biol Chem, *275:* 27909-27916, 2000.
37. Alvarez, B., Martinez, A. C., Burgering, B. M., and Carrera, A. C. Forkhead transcription factors contribute to execution of the mitotic programme in mammals. Nature, *413:* 744-747, 2001.
38. Koranda, M., Schleiffer, A., Endler, L., and Ammerer, G. Forkhead-like transcription factors recruit Ndd1 to the chromatin of G2/M-specific promoters. Nature, *406:* 94-98, 2000.
39. Ramet, M., Manfruelli, P., Pearson, A., Mathey-Prevot, B., and Ezekowitz, R. A. Functional genomic analysis of phagocytosis and identification of a Drosophila receptor for E. coli. Nature, *416:* 644-648, 2002.
40. Shankar, S., Singh, T. R., and Srivastava, R. K. Ionizing radiation enhances the therapeutic potential of TRAIL in prostate cancer in vitro and in vivo: Intracellular mechanisms. Prostate, *61:* 35-49, 2004.
41. Muller, M., Wilder, S., Bannasch, D*., et al.* p53 activates the CD95 (APO-1/Fas) gene in response to DNA damage by anticancer drugs. J Exp Med, *188:* 2033-2045, 1998.
42. Hong, Y., Muller, U. R., and Lai, F. Discriminating two classes of toxicants through expression analysis of HepG2 cells with DNA arrays. Toxicol In Vitro, *17:* 85-92, 2003.
43. de Launoit, Y., Veilleux, R., Dufour, M., Simard, J., and Labrie, F. Characteristics of the biphasic action of androgens and of the potent antiproliferative effects of the new pure antiestrogen EM-139 on cell cycle kinetic parameters in LNCaP human prostatic cancer cells. Cancer Res, *51:* 5165-5170, 1991.
44. Kokontis, J. M., Hay, N., and Liao, S. Progression of LNCaP prostate tumor cells during androgen deprivation: hormone-independent growth, repression of proliferation by androgen, and role for p27Kip1 in androgen-induced cell cycle arrest. Mol Endocrinol, *12:* 941-953, 1998.
45. Lin, H. K., Hu, Y. C., Yang, L*., et al.* Suppression versus induction of androgen receptor functions by the phosphatidylinositol 3-kinase/Akt pathway in prostate cancer LNCaP cells with different passage numbers. J Biol Chem, *278:* 50902-50907, 2003.
46. Janes, S. M., Ofstad, T. A., Campbell, D. H., Watt, F. M., and Prowse, D. M. Transient activation of FOXN1 in keratinocytes induces a transcriptional programme that promotes terminal differentiation: contrasting roles of FOXN1 and Akt. J Cell Sci, *117:* 4157-4168, 2004.
47. Zhang, X. Q., Kondrikov, D., Yuan, T. C., Lin, F. F., Hansen, J., and Lin, M. F. Receptor protein tyrosine phosphatase alpha signaling is involved in androgen depletion-induced neuroendocrine differentiation of androgen-sensitive LNCaP human prostate cancer cells. Oncogene, *22:* 6704-6716, 2003.
48. Qiu, Y., Robinson, D., Pretlow, T. G., and Kung, H. J. Etk/Bmx, a tyrosine kinase with a pleckstrin-homology domain, is an effector of phosphatidylinositol 3'-kinase and is involved in interleukin 6-induced neuroendocrine differentiation of prostate cancer cells. Proc Natl Acad Sci U S A, *95:* 3644-3649, 1998.
49. Cox, M. E., Deeble, P. D., Bissonette, E. A., and Parsons, S. J. Activated 3',5'-cyclic AMP-dependent protein kinase is sufficient to induce neuroendocrine-like differentiation of the LNCaP prostate tumor cell line. J Biol Chem, *275:* 13812-13818, 2000.

50. Lin, H. K., Wang, L., Hu, Y. C., Altuwaijri, S., and Chang, C. Phosphorylation-dependent ubiquitylation and degradation of androgen receptor by Akt require Mdm2 E3 ligase. Embo J, *21:* 4037-4048, 2002.

**Figure 1.**

**A.**

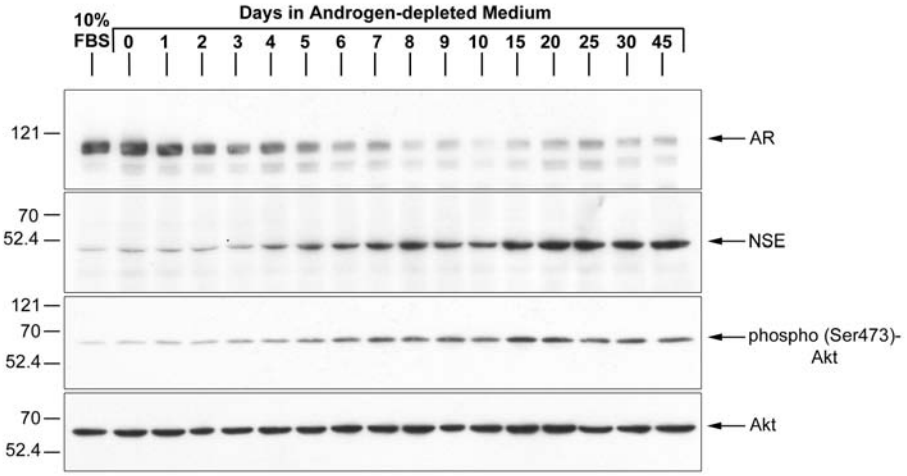


**B.**

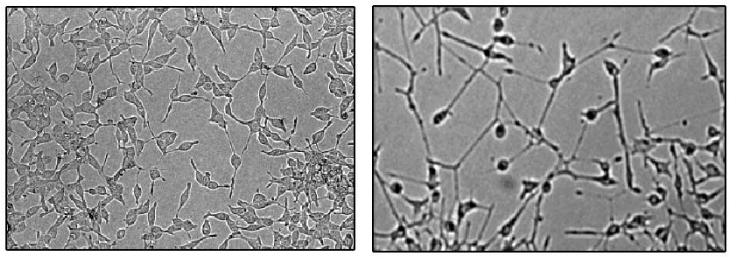

**+ Androgen (10% FBS)** **- Androgen (10% CDT-FBS)**

**Figure 2.**

**A.**

AW-repressed Genes

+DHT | -DHT (Hrs) 0.5 6 24 96

HNRNPG-T
KLK2
JIK
SEMA3C
HPGD
ELL2
IQGAP2
PRIM2A
TRG@
HPGD
CLGN
KIF22
BOP1
IQGAP2
LAMC1
MRPS12
STK39
KLK3
SLC16A6
KLK2
ACSL3
FKBP5
LDLR
GLUD2
ELL2
PTPLB
UAP1
GLUD2
DKFZP564C186
SEMA3C
KIAA0186
EIF2S1
ACTR3
HMGB2
ANXA5 a
CKS2
GMPS
DAD1
BMP2
HDAC9
DRAP1
FOS
CALU
NKX3-1
TMPRSS2
MAF
DUSP4
SSH1
TWIST1
ADRB2
GNAI1
CDC45L
KLK3
HIST1H4C
ME1
INSIG1
NOL5A
MAD2L1
X15674
VRK1
HSPC111
CDC6
CDKN3
DSCR2
PRDX4
HERC3
FEN1
FADS1
DHCR24
KLK3
KLK3
SLC1A5
KLK3
MELK
KLK3
AGR2
RRM2
KNTC2
TYMS
DDT
MYBL2
CDC6
ZWINT
S100P
AGT
ALDH1A3
KLK3
PA2G4
HLF
FEN1
OIP5
MAD2L1
SV2C
IFNA5

AW-induced Genes

+DHT | -DHT (Hrs) 0.5 6 24 96

DLX5
FZR1
NR3C1
ARHGEF2
ZNF36
ENC1
LOC155060
AF035315
CHES1
SNRK
ZNF297B
HYAL3
PLCB4
GOLPH4
PAK2
ZNF278
PTPRR
LASP1
BICD1
AL049987
SMA4
GOLGIN-67
PPP2R5B
RBL2
TLE1
THOC2
PTPRK
IGFBP3
SETBP1
IGFBP3
PPFIA2
AB002438
ZNF294
SMA5
KIAA0247
PIK3R3
STXBP5L
SMA5
BARD1
ACYP2
ZNF278
CMKOR1
SORL1
KIAA0303
MAP1B
JUN
SOX4
UGT2B11
KIAA0767
DDC
MAP1B
ACAA2
NOTCH3
CITED2
TUBA3
CD24
SERPINB5
DPYSL2
SMARCD3
SMARCD3
MDK
MDK
PIK3R3
MYRIP
TXNIP
JUN
SERPINB5
ARHGEF10
FZD2
RLN2
PLA2G2A
AUTS2
GRB10
BCHE
UGT2B15
COBL
ZNF629
U90916
PLA2G2A
CLU
UGT2B17
C5orf13
UGT2B17
SERPINI1
ARNT2
UGT2B15
IL1RN
LOC338645
LKAP
CPM

**B.**

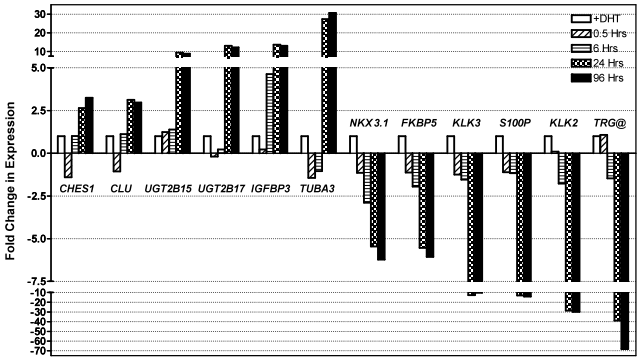


**C.**

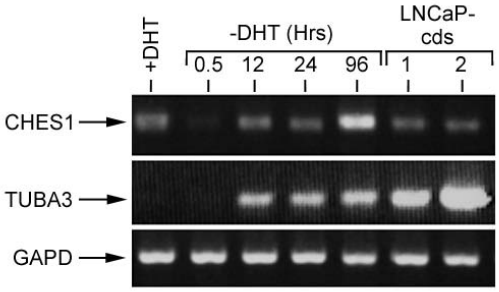


**D.**

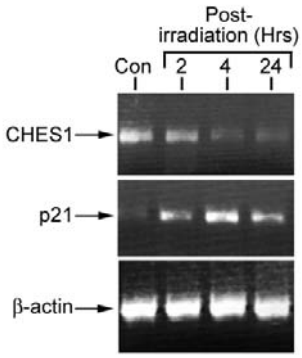

**Figure 3.**

**A.**

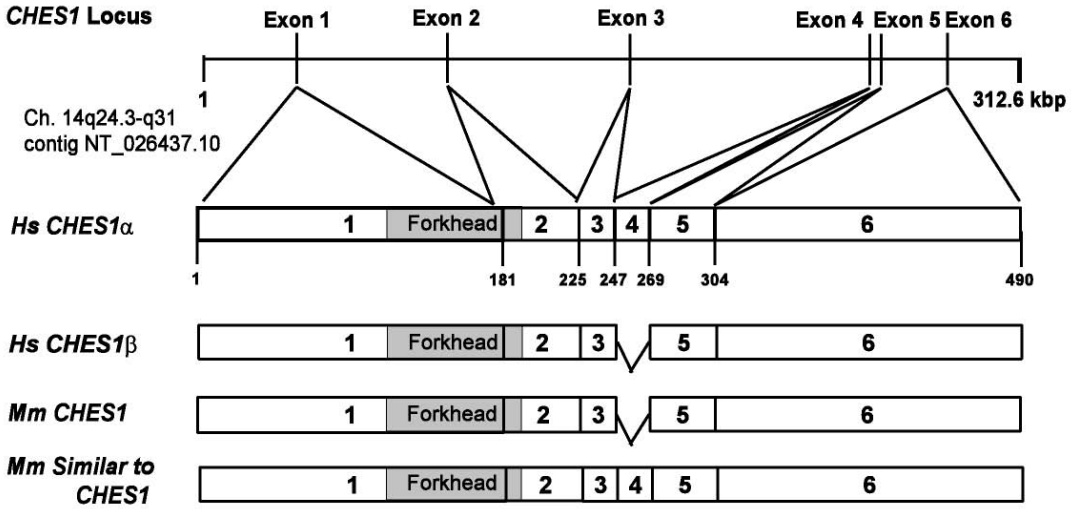


**B.**

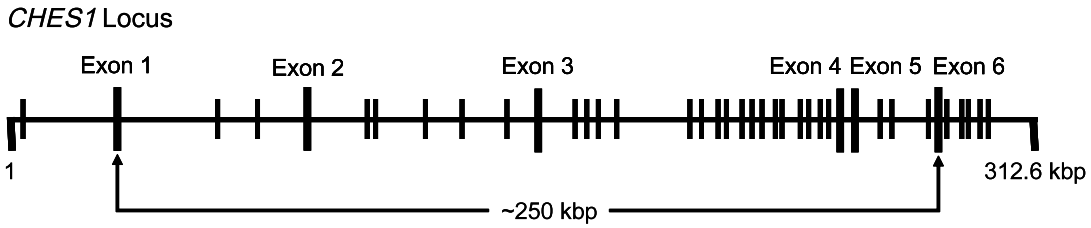


Consensus ARE/ARR sequence: (A/G)(G/T)A(A/T)C(A/T/G)nnn(A/T/G)G(T/A/C)(T/A)(C/A)(T/G/C)

**Figure 4.**

A.

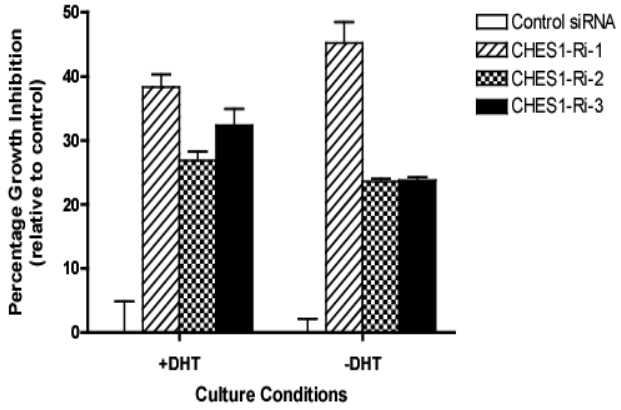
Percentage Growth Inhibition (relative to control)
50
40
30
20
10
0
+DHT
-DHT
Culture Conditions
Control siRNA
CHES1-Ri-1
CHES1-Ri-2
CHES1-Ri-3

B.

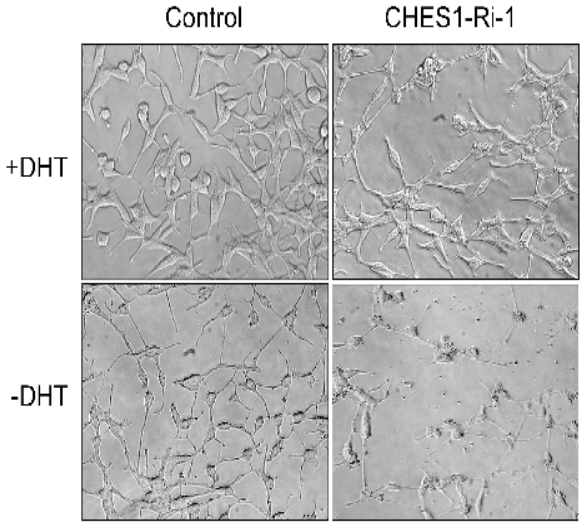
Control
CHES1-Ri-1
+DHT
-DHT

C.

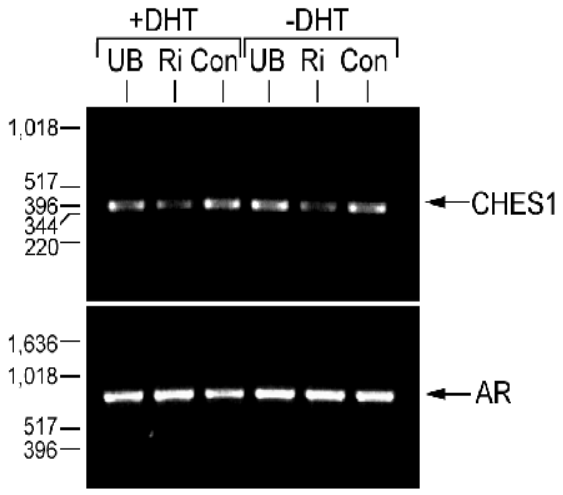
+DHT
-DHT
UB Ri Con UB Ri Con
1,018
517
396
344
220
CHES1
1,636
1,018
517
396
AR

**Figure 5.**

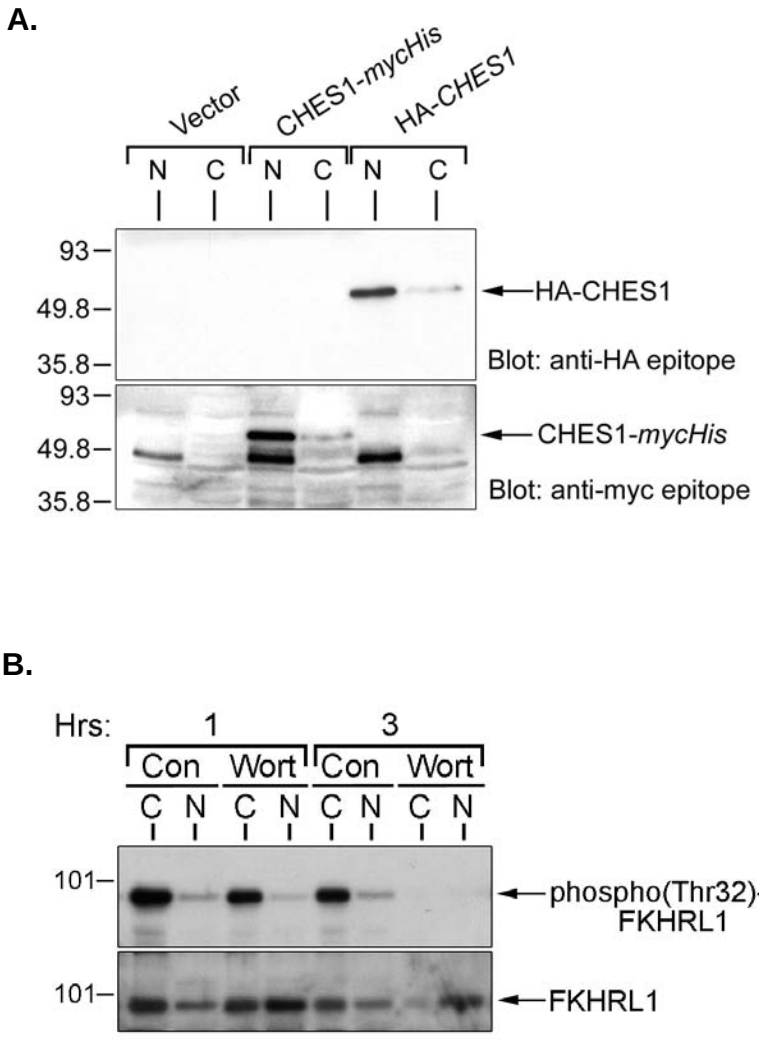
A.
Vector
CHES1-mycHis
HA-CHES1
N C N C N C
93
49.8
35.8
HA-CHES1
Blot: anti-HA epitope
93
49.8
35.8
CHES1-mycHis
Blot: anti-myc epitope
B.
Hrs: 1 3
Con Wort Con Wort
C N C N C N C N
101
phospho(Thr32)-FKHRL1
101
FKHRL1

**Figure 6.**

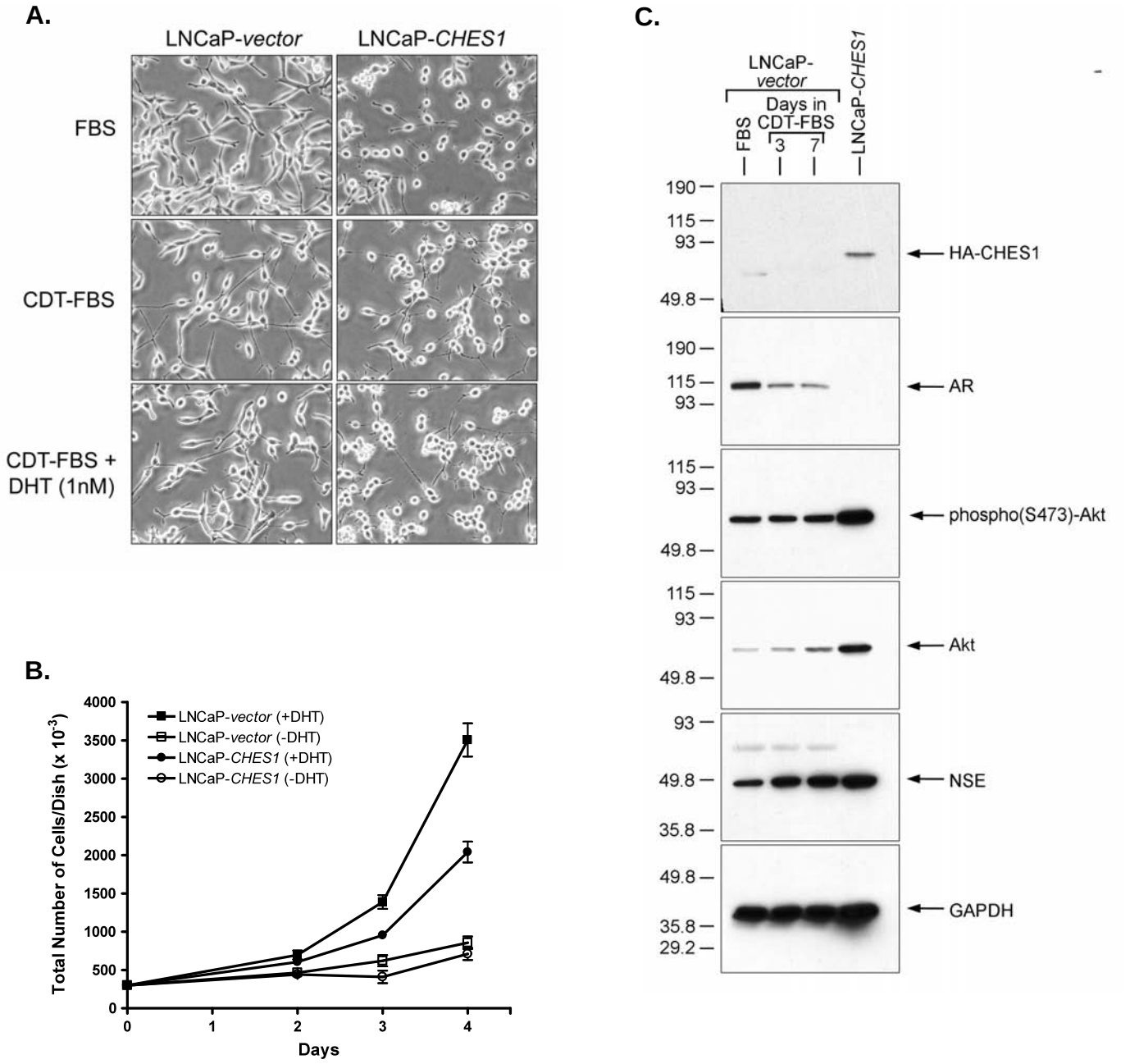
A.
LNCaP-vector
LNCaP-CHES1
FBS
CDT-FBS
CDT-FBS + DHT (1nM)
B.
LNCaP-vector (+DHT)
LNCaP-vector (-DHT)
LNCaP-CHES1 (+DHT)
LNCaP-CHES1 (-DHT)
Total Number of Cells/Dish (x 10-3)
Days
C.
LNCaP-vector
Days in CDT-FBS
FBS
3
7
LNCaP-CHES1
HA-CHES1
AR
phospho(S473)-Akt
Akt
NSE
GAPDH

**Supplementary Tables 1 and 2. Differentially expressed genes in LNCaP cells subjected to androgen deprivation.** Microarray analysis and hierarchical clustering (dChip) were performed as described in the legend to Fig. 2A and in *Materials and Methods*. The genes/transcripts comprising the AW-induced and AW-repressed gene clusters are listed in Supplementary Tables 1 and 2, respectively. Fold changes in expression at each time point (relative to the +DHT control) are shown and are statistically significant ($p$= <0.05).

**Supplementary Table 1. Up-regulated genes in LNCaP cells subjected to androgen deprivation.**

| Gene | | | Duration of androgen deprivation (Hrs)[1] | | | |
|---|---|---|---|---|---|---|
| Official Name | Symbol | Accession No. | 0.5 | 6 | 24 | 96 |
| CD24 antigen (small cell lung carcinoma cluster 4 antigen | CD24 | L33930 | 4.39 | 2.92 | 122.01 | 134.53 |
| carboxypeptidase M | CPM | J04970 | -2.24 | -1.45 | -3.41 | 53.04 |
| nuclear receptor subfamily 3, group C, member 1 (glucocorticoid receptor | NR3C1 | M10901 | 39.87 | 59.68 | 55.86 | 47.81 |
| Tubulin, alpha 3, brain-specific | TUBA3 | X01703 | -1.44 | -1.04 | 27.32 | 30.63 |
| chemokine orphan receptor 1 | CMKOR1 | U67784 | 1.93 | 2.48 | 18.29 | 19.17 |
| insulin-like growth factor binding protein 3 | IGFBP3 | M35878 | 0.22 | 4.63 | 13.69 | 13.10 |
| UDP glycosyltransferase 2 family, polypeptide B17 | UGT2B17 | U59209 | -0.19 | 0.22 | 13.05 | 12.22 |
| hypothetical protein LOC338645 | LOC338645 | X81895 | -1.19 | 1.28 | 10.47 | 10.51 |
| UDP glycosyltransferase 2 family, polypeptide B15 | UGT2B15 | U08854 | 1.24 | 1.39 | 9.46 | 8.86 |
| SMA4 | SMA4 | X83300 | 1.13 | 2.60 | 7.46 | 7.98 |
| phospholipase A2, group IIA (platelets, synovial fluid | PLA2G2A | M22430 | 1.03 | -1.13 | 8.18 | 7.85 |
| distal-less homeo box 5 | DLX5 | AC004774 | 6.53 | 5.99 | 9.38 | 6.90 |
| KIAA0303 protein | KIAA0303 | AB002301 | 1.15 | 1.67 | 6.27 | 6.69 |
| interleukin 1 receptor antagonis | IL1RN | X52015 | 1.01 | 1.29 | 6.72 | 6.55 |
| hyaluronoglucosaminidase 3 | HYAL3 | U73167 | 1.36 | 1.96 | 4.99 | 6.50 |
| UDP glycosyltransferase 2 family, polypeptide B11 | UGT2B11 | AF016492 | -1.10 | 1.20 | 5.81 | 6.12 |
| limkain b1 | LKAP | U95740 | 1.02 | 1.29 | 6.03 | 6.07 |
| Bicaudal D homolog 1 (Drosophila) | BICD1 | U90028 | 1.02 | 1.75 | 4.84 | 5.46 |
| sortilin-related receptor, L(DLR class) A repeats-containing | SORL1 | Y08110 | 1.07 | 1.33 | 4.89 | 5.22 |
| SMA5 | SMA5 | X75940 | -1.09 | 1.80 | 5.11 | 5.06 |
| frizzled homolog 2 (Drosophila) | FZD2 | L37882 | 1.56 | -1.12 | 5.27 | 4.95 |
| butyrylcholinesterase | BCHE | M16541 | 1.10 | 1.05 | 5.59 | 4.86 |
| SRY (sex determining region Y)-box 4 | SOX4 | X70683 | -1.23 | 1.27 | 4.53 | 4.68 |
| aryl-hydrocarbon receptor nuclear translocator 2 | ARNT2 | AB002305 | -1.07 | 1.10 | 4.97 | 4.66 |
| midkine (neurite growth-promoting factor 2 | MDK | X55110 | -1.48 | -1.77 | 4.53 | 4.61 |
| autism susceptibility candidate 2 | AUTS2 | AB007902 | -1.04 | 1.22 | 5.18 | 4.51 |
| golgin-67 | GOLGIN-67 | AB020662 | -1.01 | 1.75 | 4.11 | 4.51 |
| relaxin 2 (H2) | RLN2 | X00948 | -1.06 | -1.05 | 5.46 | 4.50 |
| growth factor receptor-bound protein 10 | GRB10 | D86962 | -1.00 | 1.12 | 5.21 | 4.49 |
| microtubule-associated protein 1B | MAP1B | W27148 | -1.07 | 1.35 | 4.11 | 4.43 |
| cordon-bleu homolog (mouse) | COBL | AB014533 | 1.07 | 1.05 | 4.93 | 4.41 |
| fizzy/cell division cycle 20 related 1 (Drosophila) (Fzr1 protein | FZR1 | AA932443 | 4.28 | 5.19 | 3.96 | 4.31 |
| acylphosphatase 2, muscle type | ACYP2 | X84195 | -1.81 | 1.06 | 4.16 | 4.30 |
| myosin VIIA and Rab interacting protein | MYRIP | AL050090 | 1.29 | 1.56 | 5.25 | 4.19 |
| serine (or cysteine) proteinase inhibitor, clade I (neuroserpin), member | SERPINI1 | Z81326 | -1.08 | 1.04 | 4.34 | 4.11 |
| Notch homolog 3 (Drosophila) | NOTCH3 | U97669 | -1.28 | -1.08 | 3.91 | 4.03 |
| dihydropyrimidinase-like 2 | DPYSL2 | U97105 | -1.25 | 1.03 | 3.60 | 4.00 |
| transducin-like enhancer of split 1 (E(sp1) homolog, Drosophila) | TLE1 | M99435 | -1.07 | 1.86 | 3.47 | 3.96 |
| PTPRF interacting protein (liprin) alpha 2 | PPFIA2 | AF034799 | 1.10 | 2.06 | 4.09 | 3.85 |
| acetyl-Coenzyme A acyltransferase 2 | ACAA2 | D16294 | 1.05 | 1.27 | 3.29 | 3.67 |
| zinc finger protein 629 | ZNF629 | AB002324 | 1.18 | 1.02 | 3.71 | 3.65 |
| Cbp/p300-interacting transactivator, with Glu/Asp-rich C-terminal domain, 2 | CITED2 | U65093 | -1.23 | -1.15 | 3.55 | 3.64 |
| golgi phosphoprotein 4 | GOLPH4 | AI126171 | -1.40 | 1.42 | 2.91 | 3.59 |
| SWI/SNF-related matrix-associated actin-dependent regulator of chromatin d3 | SMARCD3 | U66619 | -1.18 | -1.23 | 3.17 | 3.56 |
| v-jun sarcoma virus 17 oncogene homolog (avian) | JUN | J04111 | 1.12 | 1.34 | 4.01 | 3.54 |
| KIAA0247 gene product | KIAA0247 | D87434 | -1.08 | 1.40 | 3.68 | 3.51 |
| SNF-1 related kinase | SNRK | D43636 | 1.02 | 1.10 | 2.89 | 3.47 |
| protein tyrosine phosphatase, receptor type, F | PTPRR | D64053 | 1.01 | 1.61 | 3.08 | 3.44 |
| p21 (CDKN1A)-activated kinase 2 | PAK2 | U24153 | 1.43 | 1.58 | 3.03 | 3.43 |
| ectodermal-neural cortex (with BTB-like domain | ENC1 | AF059611 | 1.61 | 2.00 | 4.02 | 3.42 |
| SMA5 | SMA5 | X83301 | -1.28 | 1.39 | 3.60 | 3.41 |
| zinc finger protein 278 | ZNF278 | AL096880 | -1.35 | 1.10 | 3.19 | 3.40 |
| v-jun sarcoma virus 17 oncogene homolog (avian) | JUN | J04111 | -1.02 | 1.21 | 3.19 | 3.36 |
| protein tyrosine phosphatase, receptor type, K | PTPRK | L77886 | 1.32 | 1.63 | 3.25 | 3.35 |
| phospholipase A2, group IIA (platelets, synovial fluid | PLA2G2A | M22430 | -1.07 | -1.09 | 3.88 | 3.28 |
| chromosome 5 open reading frame 13 | C5orf13 | U30521 | -1.04 | 1.05 | 3.51 | 3.27 |
| checkpoint suppressor 1 | CHES1 | U68723 | -1.41 | 1.01 | 2.65 | 3.25 |
| zinc finger protein 36 (KOX 18 | ZNF36 | U09848 | 1.32 | 1.82 | 3.72 | 3.24 |
| hypothetical protein LOC155060 | LOC155060 | AF035281 | 1.51 | 1.64 | 3.97 | 3.23 |
| phospholipase C, beta 4 | PLCB4 | L41349 | -1.08 | 1.19 | 2.36 | 3.22 |
| zinc finger protein 278 | ZNF278 | AI352450 | -1.03 | 1.43 | 2.73 | 3.17 |
| THO complex 2 | THOC2 | AA928996 | 1.29 | 1.63 | 3.10 | 3.11 |
| KIAA0767 protein | KIAA0767 | AB018310 | -1.07 | 1.13 | 2.93 | 3.09 |
| syntaxin binding protein 5-like | STXBP5L | AB023223 | 1.05 | 1.40 | 3.05 | 3.08 |
| serine (or cysteine) proteinase inhibitor, clade B (ovalbumin), member 5 | SERPINB5 | U04313 | -0.01 | 0.16 | 3.17 | 3.05 |
| LIM and SH3 protein 1 | LASP1 | X82456 | -1.15 | 1.36 | 2.84 | 3.03 |
| rho/rac guanine nucleotide exchange factor (GEF) 2 | ARHGEF2 | AB014551 | 1.74 | 1.58 | 2.92 | 3.01 |
| clusterin (CLI, SP-40, SGP-2, TRPM-2, apolipoprotein J) | CLU | M25915 | -1.06 | 1.12 | 3.13 | 2.97 |
| protein phosphatase 2, regulatory subunit B (B56), beta isoform | PPP2R5B | L42374 | 1.16 | 1.62 | 2.63 | 2.97 |
| SET binding protein 1 | SETBP1 | AB022660 | 1.08 | 1.55 | 3.04 | 2.95 |
| dopa decarboxylase (aromatic L-amino acid decarboxylase) | DDC | M76180 | -1.07 | 1.11 | 2.81 | 2.92 |
| thioredoxin interacting protein | TXNIP | S73591 | 1.21 | 1.46 | 3.16 | 2.91 |
| retinoblastoma-like 2 (p130) | RBL2 | X74594 | 1.04 | 1.61 | 2.57 | 2.84 |
| phosphoinositide-3-kinase, regulatory subunit, polypeptide 3 (p55, gamma | PIK3R3 | D88532 | -0.01 | 1.24 | 3.26 | 2.82 |
| Rho guanine nucleotide exchange factor (GEF) 10 | ARHGEF10 | AB002292 | 1.23 | 1.12 | 2.99 | 2.79 |
| zinc finger protein 297B | ZNF297B | AB007874 | 1.11 | 1.25 | 2.30 | 2.74 |
| zinc finger protein 294 | ZNF294 | AB018257 | -1.21 | 1.38 | 2.69 | 2.74 |
| BRCA1 associated RING domain 1 | BARD1 | U76638 | -1.09 | 1.39 | 2.78 | 2.72 |

[1]Values are fold changes in expression relative to LNCaP cultured in the presence of DHT and are statistically significant based upon $p$ = <0.05

**Supplementary Table 2. Down-regulated genes in LNCaP cells subjected to androgen deprivation.**

| Gene | | | Duration of androgen deprivation (Hrs)[1] | | | |
|---|---|---|---|---|---|---|
| Official Name | Symbol | Accession No. | 0.5 | 6 | 24 | 96 |
| anterior gradient 2 homolog (Xenopus laevis) | AGR2 | AF038451 | -1.13 | -1.11 | -2.66 | -2.69 |
| Glutamate dehydrogenase-2 | GLUD2 | U08997 | -1.19 | -1.59 | -2.88 | -2.71 |
| thymidylate synthetase | TYMS | X02308 | -1.18 | -1.13 | -2.68 | -2.71 |
| D-dopachrome tautomerase | DDT | U49785 | -1.16 | -1.19 | -2.64 | -2.76 |
| eukaryotic translation initiation factor 2, subunit 1 alpha, 35kDa | EIF2S1 U26032 | | -1.29 | -1.48 | -3.22 | -2.79 |
| maternal embryonic leucine zipper kinase | MELK D79997 | | 1.03 | 1.04 | -2.99 | -2.80 |
| mitochondrial ribosomal protein S12 | MRPS12 | Y11681 | -1.14 | -1.31 | -2.65 | -2.80 |
| ARP3 actin-related protein 3 homolog (yeast) | ACTR3 | AF006083 | -1.31 | -1.50 | -2.56 | -2.83 |
| 24-dehydrocholesterol reductase | DHCR24 D13643 | | 1.01 | -1.04 | -2.89 | -2.83 |
| laminin, gamma 1 (formerly LAMB2) | LAMC1 | M55210 | -1.12 | -1.39 | -3.00 | -2.85 |
| histone 1, H4c | HIST1H4C | AA255502 | -1.38 | 1.02 | -2.93 | -2.86 |
| block of proliferation 1 | BOP1 | D50914 | -1.15 | -1.42 | -3.05 | -2.88 |
| nucleolar protein 5A (56kDa with KKE/D repeat) | NOL5A | Y12065 | -1.38 | -1.14 | -3.16 | -2.89 |
| annexin A5 | ANXA5 a | U05770 | -1.34 | -1.86 | -3.38 | -2.91 |
| vaccinia related kinase 1 | VRK1 | AB000449 | -1.32 | -1.25 | -3.29 | -2.93 |
| ZW10 interactor | ZWINT | AF067656 | -1.11 | -1.16 | -2.96 | -2.99 |
| solute carrier family 1 (neutral amino acid transporter), member 5 | SLC1A5 U53347 | | 1.07 | 1.04 | -2.85 | -2.99 |
| peroxiredoxin 4 | PRDX4 | U25182 | -1.38 | -1.34 | -3.12 | -2.99 |
| PTP-like (proline instead of catalytic arginine), member b | PTPLB | AF052159 | -1.26 | -1.69 | -3.27 | -3.01 |
| proliferation-associated 2G4, 38kD | PA2G4 | U59435 | -1.20 | -1.08 | -4.17 | -3.05 |
| calumenin | CALU | AF013759 | -1.13 | -1.92 | -2.81 | -3.06 |
| primase, polypeptide 2A (58kD) | PRIM2A | X74331 | 1.05 | -1.31 | -2.88 | -3.07 |
| v-maf musculoaponeurotic fibrosarcoma oncogene homolog (avian) | MAF | AF055376 | -1.07 | -2.88 | -3.03 | -3.13 |
| acyl-CoA synthetase long-chain family member 3 | ACSL3 | AA977580 | -1.12 | -1.79 | -3.42 | -3.14 |
| high-mobility group box 2 | HMGB2 | X62534 | -1.31 | -1.57 | -3.00 | -3.14 |
| low density lipoprotein receptor (familial hypercholesterolemia) | LDLR L00352 | | -1.09 | -1.66 | -3.34 | -3.15 |
| CDC6 cell division cycle 6 homolog (S. cerevisiae) | CDC6 | U77949 | -1.28 | -1.18 | -3.98 | -3.16 |
| defender against cell death 1 | DAD1 | D15057 | -1.26 | -2.03 | -3.45 | -3.19 |
| malic enzyme 1, NADP(+)-dependent, cytosolic | ME1 | AL049699 | -1.34 | -1.13 | -3.50 | -3.21 |
| hypothetical protein HSPC111 | HSPC111 | AI553745 | -1.27 | -1.18 | -3.36 | -3.22 |
| flap structure-specific endonuclease 1 | FEN1 | X76771 | -1.09 | -0.03 | -3.53 | -3.22 |
| aldehyde dehydrogenase 1 family, member A3 | ALDH1A3 U07919 | | -1.05 | -1.15 | -3.65 | -3.23 |
| Opa-interacting protein 5 | OIP5 | AF025441 | -1.11 | 1.04 | -3.30 | -3.26 |
| DR1-associated protein 1 (negative cofactor 2 alpha) | DRAP1 | U41843 | -1.48 | -2.53 | -3.03 | -3.27 |
| kinesin family member 22 | KIF22 | AB017430 | -1.10 | -1.50 | -3.54 | -3.39 |
| DKFZP564C186 protein | DKFZP564C186 | AL050019 | -1.32 | -1.69 | -3.40 | -3.42 |
| Down syndrome critical region gene 2 | DSCR2 | AJ006291 | -1.55 | -1.28 | -3.24 | -3.43 |
| fatty acid desaturase 1 | FADS1 | AC004770 | 1.04 | -1.02 | -3.16 | -3.44 |
| KIAA0186 gene product | KIAA0186 | D80008 | -1.24 | -1.56 | -3.56 | -3.49 |
| v-myb myeloblastosis viral oncogene homolog (avian)-like 2 | MYBL2 | X13293 | -1.21 | -1.24 | -4.11 | -3.63 |
| insulin induced gene 1 | INSIG1 | U96876 | -1.34 | -1.11 | -4.37 | -3.69 |
| Glutamate dehydrogenase-2 | GLUD2 | U08997 | -1.28 | -1.79 | -3.34 | -3.71 |
| IQ motif containing GTPase activating protein 2 | IQGAP2 | U51903 | 0.00 | -1.38 | -4.06 | -3.82 |
| cyclin-dependent kinase inhibitor 3 | CDKN3 | L25876 | -1.35 | -1.20 | -4.55 | -3.85 |
| STE20-like kinase | JIK | AA576724 | 1.05 | -1.64 | -4.25 | -3.91 |
| kinetochore associated 2 | KNTC2 | AF017790 | -1.24 | -1.18 | -3.58 | -3.93 |
| MAD2 mitotic arrest deficient-like 1 (yeast) | MAD2L1 | U65410 | -1.30 | -0.11 | -4.34 | -3.98 |
| adrenergic, beta-2-, receptor, surface | ADRB2 | M15169 | -1.07 | -2.81 | -4.40 | -4.00 |
| interferon, alpha 5 | IFNA5 | X02956 | 1.04 | -1.15 | -1.94 | -4.10 |
| dual specificity phosphatase 4 | DUSP4 | U48807 | -1.17 | -3.14 | -5.33 | -4.15 |
| angiotensinogen (serine (or cysteine) proteinase inhibito | AGT K02215 | | -1.12 | -1.16 | -4.88 | -4.17 |
| hect domain and RLD 3 | HERC3 | D25215 | -1.06 | -1.00 | -5.60 | -4.40 |
| ribonucleotide reductase M2 polypeptide | RRM2 | X59618 | -1.22 | -1.13 | -5.14 | -4.57 |
| G protein alpha inhibiting activity polypeptide | GNAI1 | AL049933 | -1.13 | 1.33 | -6.40 | -4.82 |
| UDP-N-acteylglucosamine pyrophosphorylase 1 | UAP1 | AB011004 | -1.31 | -1.92 | -6.19 | -4.83 |
| CDC45 cell division cycle 45-like (S. cerevisiae) | CDC45L | AJ223728 | 1.06 | 1.34 | -5.36 | -5.05 |
| guanine monphosphate synthetase | GMPS | U10860 | -1.31 | -2.48 | -6.04 | -5.09 |
| testes-specific heterogenous nuclear ribonucleoprotein G-T | HNRNPG-T | AF069682 | -1.82 | -6.21 | -2.34 | -5.12 |
| calmegin | CLGN | D86322 | -1.08 | -1.33 | -5.27 | -5.30 |
| histone deacetylase 9 | HDAC9 | AB018287 | -1.56 | -5.37 | -4.62 | -5.38 |
| solute carrier family 16 (monocarboxylic acid transporters), member 6 | SLC16A6 | U79745 | -1.08 | -1.80 | -6.92 | -5.49 |
| CDC28 protein kinase regulatory subunit 2 | CKS2 | X54942 | -1.29 | -2.64 | -6.01 | -6.03 |
| FK506-binding protein 5 | FKBP5 | U42031 | -1.13 | -1.95 | -5.54 | -6.06 |
| NK3 transcription factor related, locus 1 (Drosophila) | NKX3-1 | U80669 | -1.14 | -2.89 | -5.45 | -6.22 |
| CDC6 cell division cycle 6 homolog (S. cerevisiae) | CDC6 | U77949 | -1.01 | -1.10 | -5.30 | -6.31 |
| serine threonine kinase 39 (STE20/SPS1 homolog, yeast) | STK39 | AF099989 | -1.29 | -1.53 | -7.87 | -6.83 |
| transmembrane protease, serine 2 | TMPRSS2 | U75329 | -1.09 | -4.65 | -7.71 | -7.54 |
| kallikrein 3, (prostate specific antigen), Alt. Splice Form 2 | KLK3 | M21896 | -0.02 | -1.07 | -11.11 | -7.86 |
| elongation factor, RNA polymerase II, 2 | ELL2 | U88629 | -1.17 | -1.81 | -11.15 | -8.06 |
| bone morphogenetic protein 2 | BMP2 | M22489 | -2.04 | -12.49 | -22.68 | -8.35 |
| semaphorin 3C | SEMA3C | AB000220 | -1.27 | -1.93 | -9.81 | -8.64 |
| twist homolog 1 (Drosophila) | TWIST1 | X99268 | -1.04 | -3.67 | -10.01 | -9.24 |
| v-fos FBJ murine osteosarcoma viral oncogene homolog | FOS | V01512 | -1.27 | -13.83 | -13.27 | -9.53 |
| kallikrein 3, (prostate specific antigen | KLK3 | X07730 | -1.25 | -1.54 | -12.64 | -10.30 |
| slingshot 1 | SSH1 | W28356 | -1.13 | -3.98 | -94.74 | -11.29 |
| synaptic vesicle glycoprotein 2C | SV2C | AB028977 | -1.45 | -1.42 | -2.91 | -12.22 |
| hepatic leukemia factor | HLF | M95585 | -1.26 | -1.02 | -7.60 | -14.00 |
| S100 calcium binding protein P | S100P | AA131149 | -1.11 | -1.17 | -12.95 | -14.17 |
| hydroxyprostaglandin dehydrogenase 15-(NAD) | HPGD | L76465 | -1.02 | -1.60 | -20.03 | -28.79 |
| kallikrein 2, prostatic | KLK2 | S39329 | 0.09 | -1.77 | -28.68 | -29.91 |
| T cell receptor gamma locus | TRG@ | M30894 | 1.07 | -1.47 | -38.80 | -68.24 |

[1]Values are fold changes in expression relative to LNCaP cultured in the presenceof DHT and are statistically significant based upon $p$ = <0.05

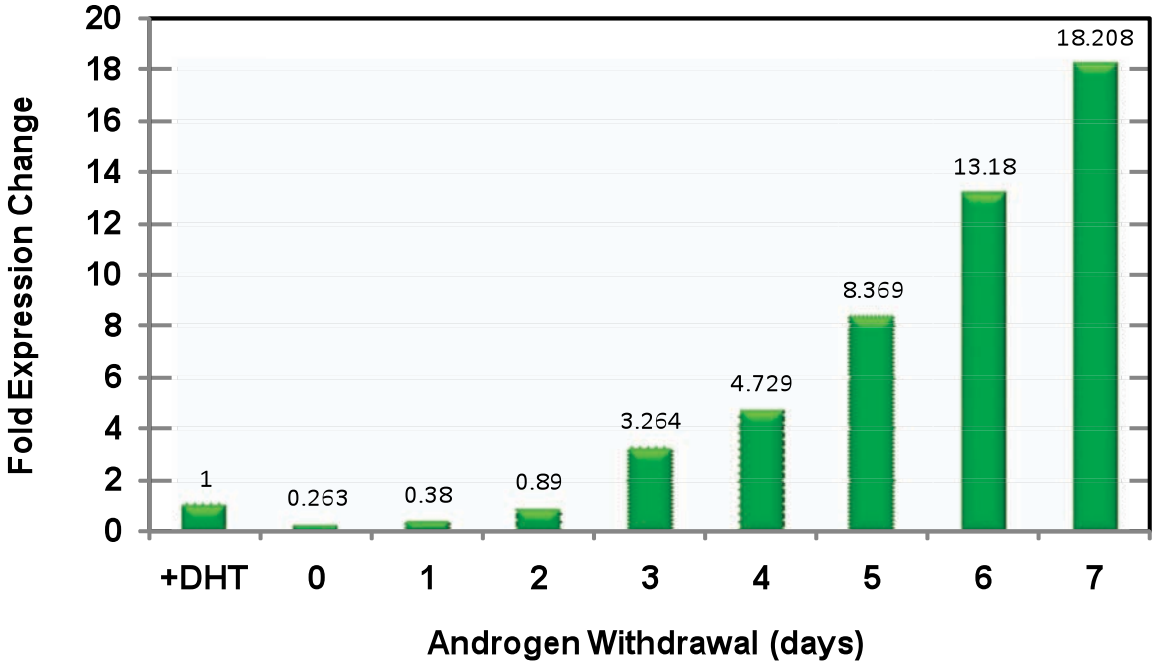


**Figure 1.** *CHES1* expression is induced by androgen withdrawal. LNCaP cells were cultured in the presence of DHT (1nM, 7 days) or subjected to androgen deprivation for 0-7 days by shifting the cultures to medium supplemented with charcoal/dextran-treated FBS (CDT-FBS). At each time point, the cells were harvested for isolation of total RNA using the RNeasy kit (Qiagen). Subsequently, *CHES1* transcript levels were determined using quantitative RT-PCR (qRT-PCR) with specific TaqMan gene expression assays (Applied Biosystems). All results were normalized to the expression of *GAPDH* in each sample. Fold changes in *CHES1* expression at each time point were calculated relative to that of the DHT-treated sample.

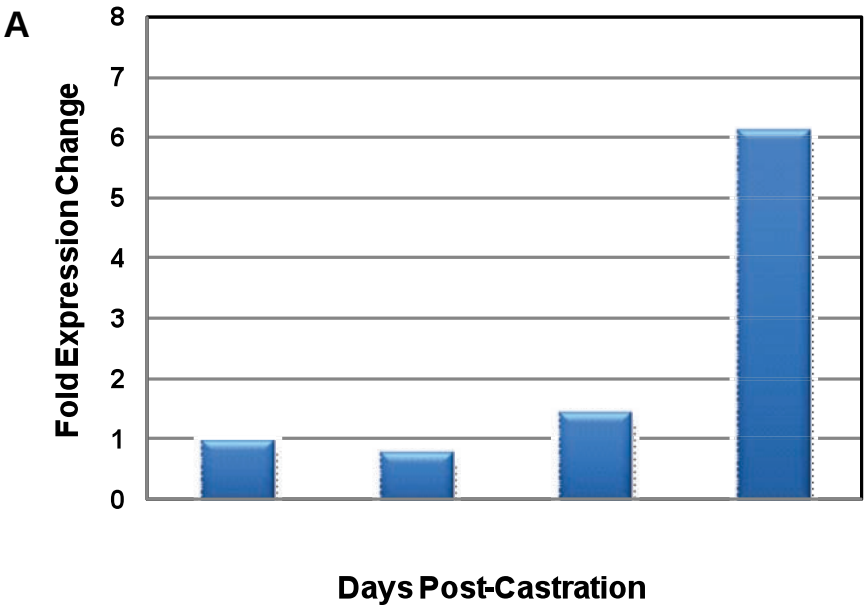


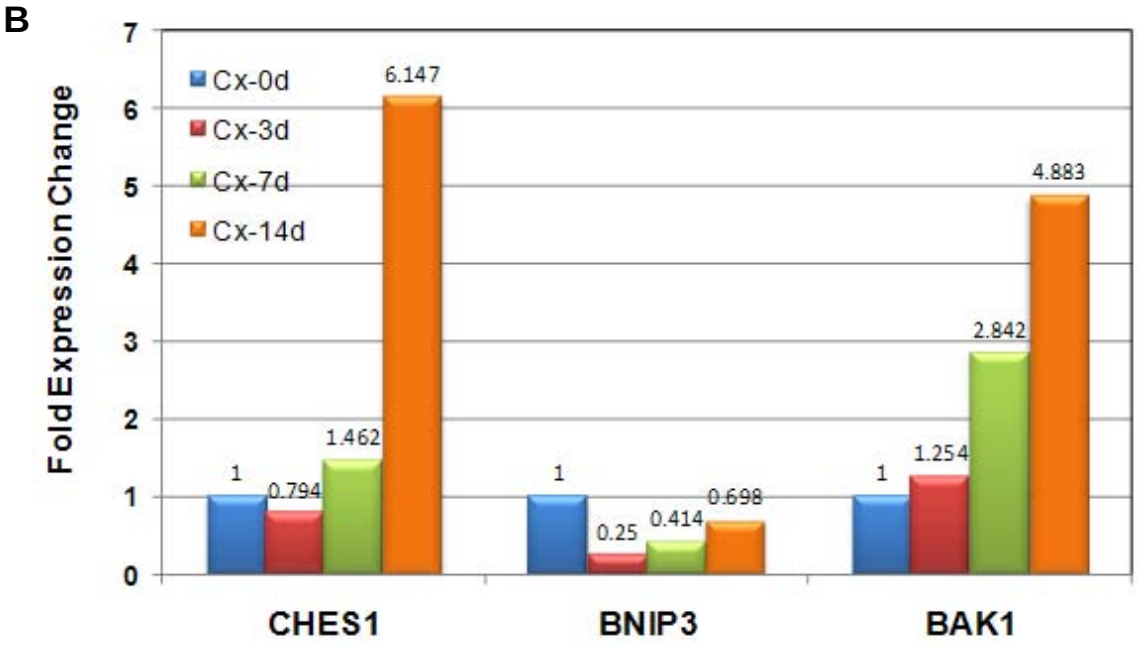


**Figure 2.** *CHES1* gene expression is induce in vivo in an experimental model of androgen deprivation. CWR22 xenografts were established in male, nude athymic mice by subcutaneous injection of a suspension of 2.5 x $10^6$ cells in Matrigel basement mebrane matrix (BD Pharmingen). Three days prior to injection, each mouse was implanted with a 90-day sustained-release testosterone pellet (12.5 mg). When the tumors reached a size of 0.5-$cm^3$, androgen ablation was initiated by castration (Cx) of the mice (*i.e.*, bilateral orchiectomy). At 0, 3, 7, and 14 days post-castration, mice were sacrificed and the tumors harvested. Total RNA was prepared and qRT-PCR performed as described in the legend to Figure 1. ***A)*** Castration-induced changes in *CHES1* expression are depicted in relation to expression in xenografts from intact mice (Day 0). ***B)*** In the same study, qRT-PCR analyses were also performed to examine the expression of the pro-apoptotic Bcl-2 family members BNIP3 and BAK1.

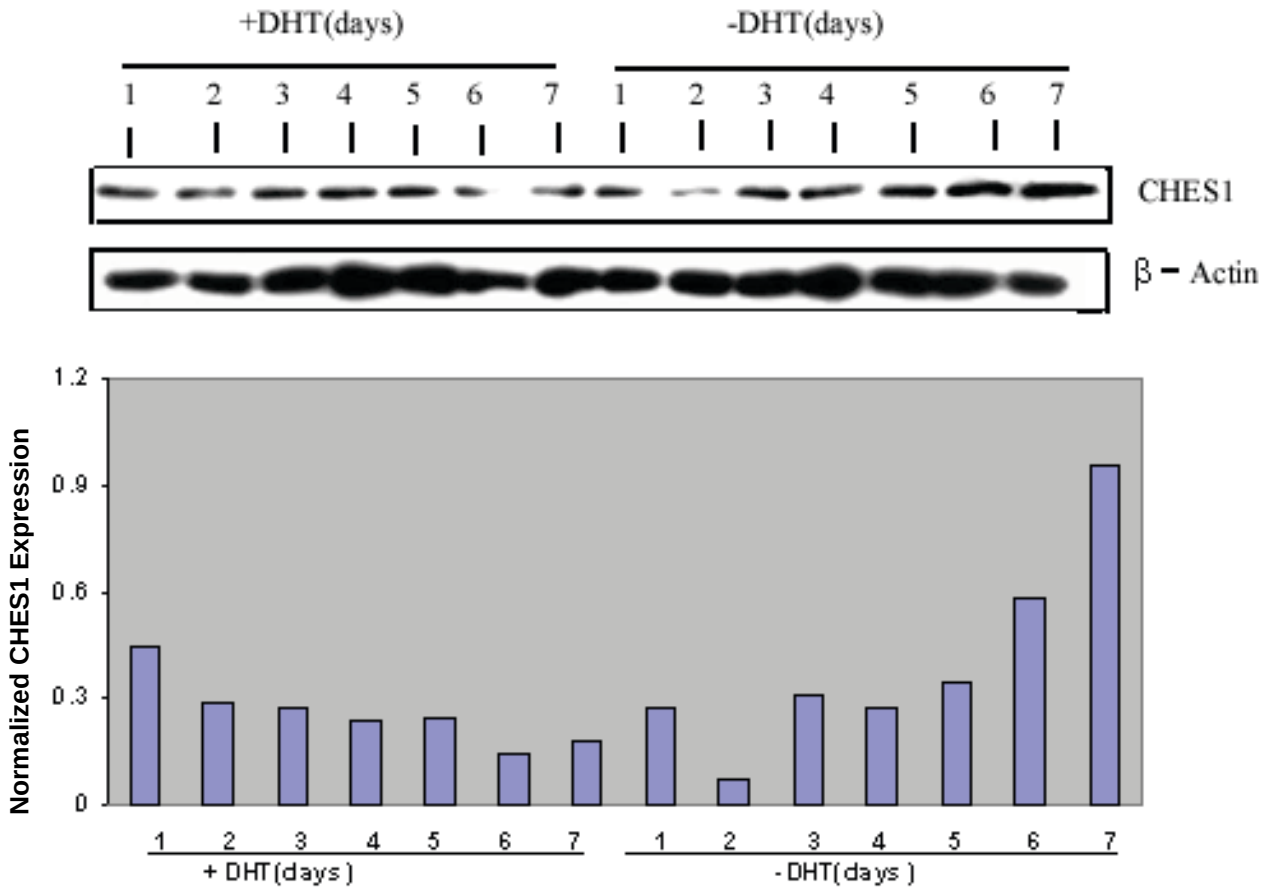


**Figure 3.** CHES1 protein levels are persistently elevated in response to androgen withdrawal. LNCaP cells (1.5 x $10^6$) were seeded into 10-cm tissue culture dishes and cultured in the presence of androgen ***(+DHT)*** or subjected to androgen withdrawal ***(-DHT)*** for 0-7 days. At each time point, cells were harvested, lysed in RIPA buffer, and analyzed by immunoblot analysis for the expression of CHES1 protein (*top panel*). The same blots were also probed for the expression of β-actin as a normalization control. Normalized CHES1 expression levels (*i.e.*, using β-actin) in each sample are depicted by the graph in the bottom panel.

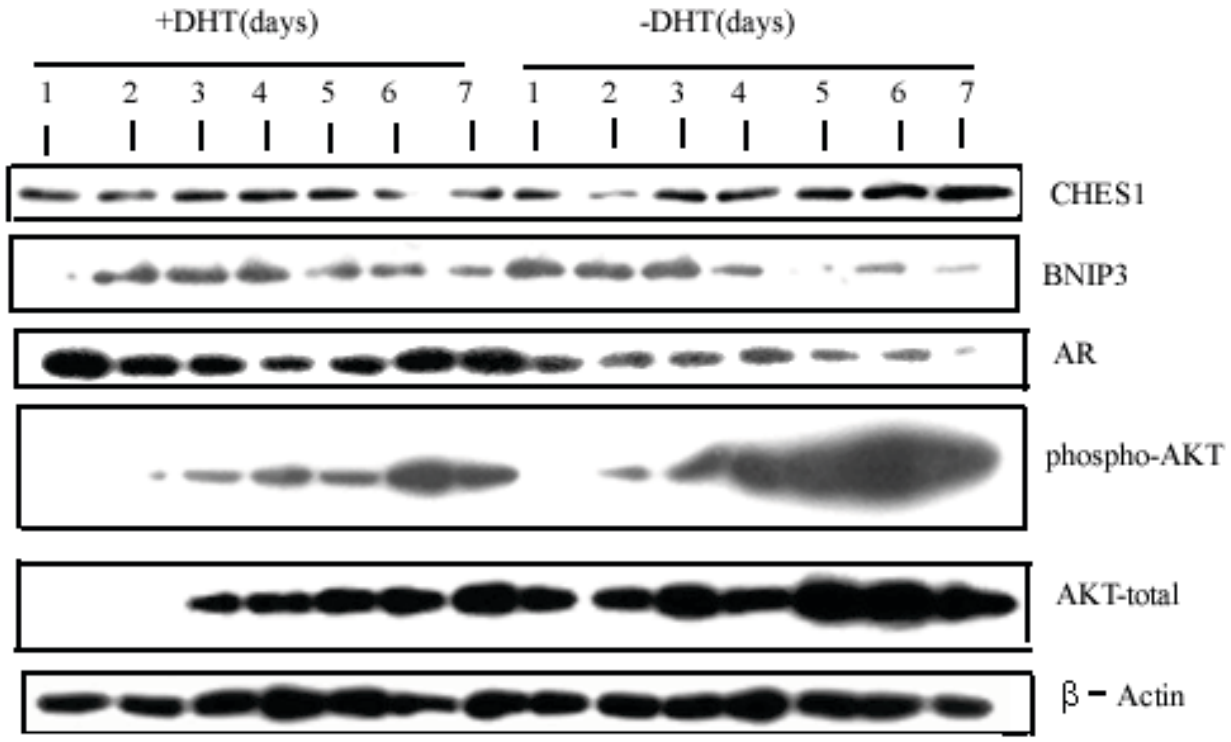


**Figure 4.** Androgen withdrawal mediates coordinated expression changes of CHES1 and regulators of apoptosis. Protein lysates from the experiment described in Figure 3 were also analyzed for the levels of Ser473-phosphorylated Akt and expression of BNIP3, AR, and total Akt.

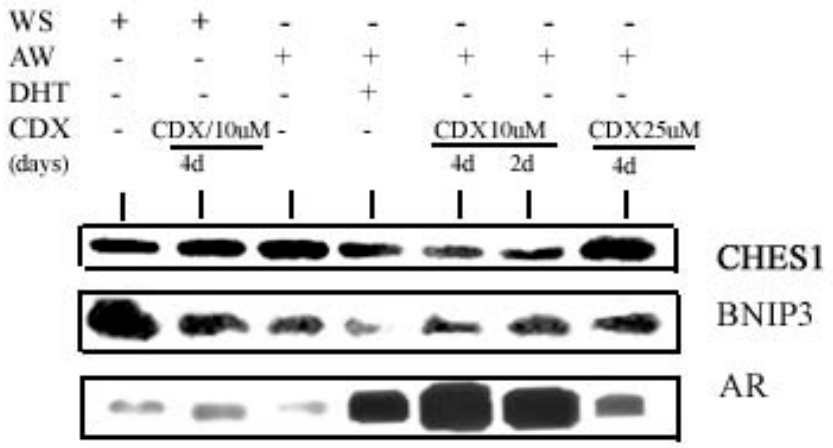


**Figure 5.** CHES1 expression is induced in response to combined androgen ablation. LNCaP cells (1.5 x $10^6$)were seeded into 60-mm tissue culture dishes and cultured in complete medium containing FBS, subjected to androgen withdrawal (AW) by supplementation of the medium with CDT-FBS. Androgen-sufficient conditions were restored in one sample by adding DHT (1 nM). Combined androgen ablation was simulated by the addition of Casodex (Cdx) at the indicated concentrations. The cells were harvested and lysed in RIPA buffer. Immunoblot analysis was performed for the evaluation of CHES1, BNIP3, and AR expression.

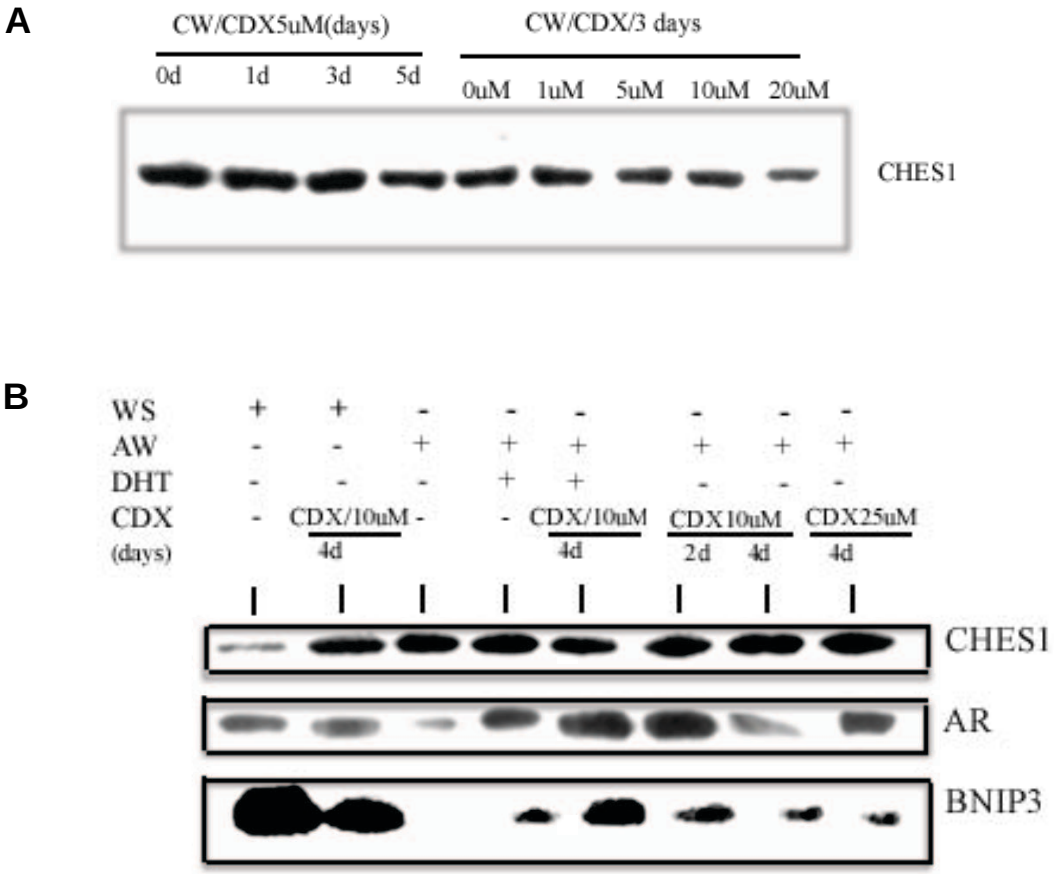


**Figure 6.** Modulation of CHES1 expression by androgen ablation in the CWR22Pc cell model. ***A)*** A time-course and dose-response pilot experiment was performed in order to better define the parameters which should be used for subsequent experiments aimed at determining the regulation of CHES1 expression in CWR22Pc cells in response to treatment with Casodex (CdX). CWR22Pc is a new androgen-sensitive cell line derived from the androgen-dependent CWR22 xenograft. For this experiment, cells were treated for the indicated durations with 5-µM Cdx or for 3 days with a range of concentrations from 0-20 µM. The cultures were harvested in RIPA lysis buffer and immunoblot analysis was performed for the expression of CHES1. ***B)*** A similar experiment to that performed with LNCaP cells (Fig. 5) was performed with CWR22Pc cells. Cells ($2.5 \times 10^6$) were seeded into 60 mm dishes and treated as described in Figure 5 above. In addition, the ability of Cdx to antagonize the effects of androgen was tested by including a combination treatment of the two agents. Cells were harvested, lysed, and analyzed by immunoblot analysis as described above.

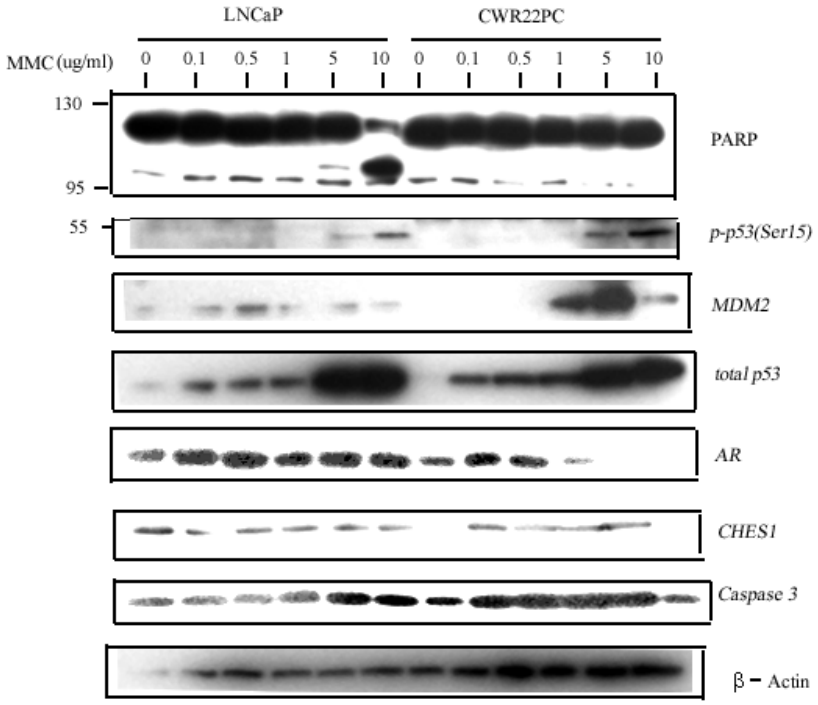


**Figure 7.** Mitomycin C (MMC) treatment down-regulates *CHES1* expression. LNCaP (1.5 x $10^6$) and CWR22 (2.5 x $10^6$) cells were seeded into 60-mm tissue culture dishes in complete medium (RPMI 1640/10% FBS/L-Glu). For CWR22Pc, DHT (0.8 nM) was added to the medium. The cells were then were treated with the indicated concentrations of mitomycin C (0.1-10 µg/ml) or vehicle. Twenty-four hours later, cultures were harvested and lysed in RIPA buffer. Immunoblot analysis was then performed to evaluate the expression of the indicated proteins.

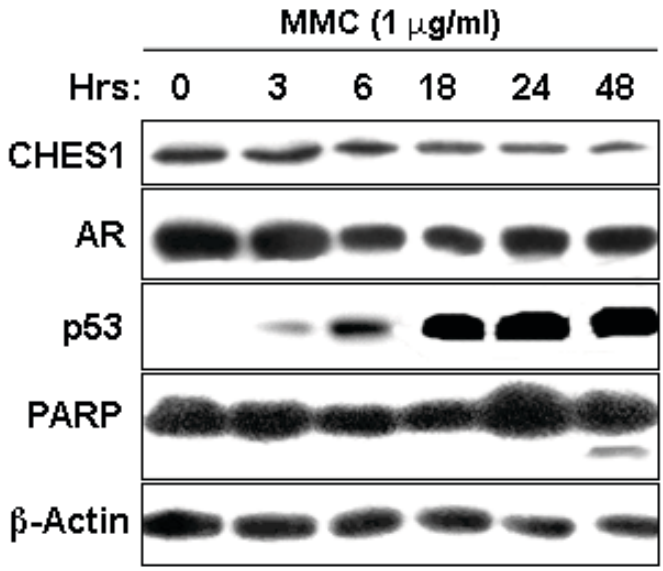


**Figure 8.** *CHES1* expression is down-regulated in response to genotoxic stress. LNCaP cells (1.5 x $10^6$) were seeded into 60-mm tissue culture dishes in complete medium (RPMI 1640/10% FBS/L-Glu). Twenty-four hours later, the cells were treated with mitomycin C (MMC; 1 μg/ml) and harvested at the indicated times from 0 to 48 hours. The cells were lysed in RIPA lysis buffer. Immunoblot analysis was then performed to evaluate the expression of the indicated proteins.

**A**

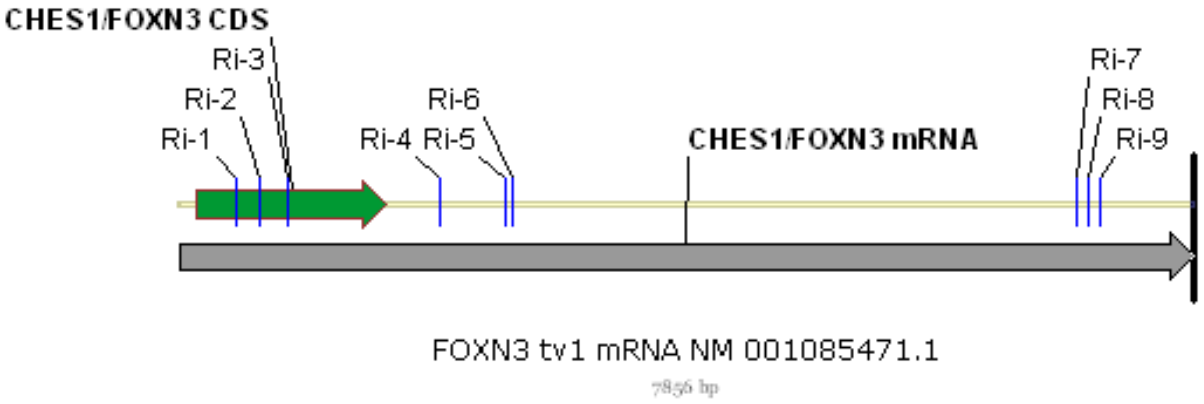


**B**

| Name of shRNA | Location of Site Targeted by shRNA (base numbers) | | | Description | |
|---|---|---|---|---|---|
| | | | | Source | Clone Number |
| **CHES1-Ri-1** | 431 | - | 452 | Custom-designed | NA |
| **CHES1-Ri-2** | 615 | - | 636 | Custom-designed | NA |
| **CHES1-Ri-3** | 841 | - | 862 | Custom-designed | NA |
| **CHES1-Ri-4** | 2,024 | - | 2,044 | Open Biosystems | shRNA Clone V2HS_48273 |
| **CHES1-Ri-5** | 2,532 | - | 2,552 | Open Biosystems | shRNA Clone V2HS_48274 |
| **CHES1-Ri-6** | 2,572 | - | 2,592 | Open Biosystems | shRNA Clone V2HS_48276 |
| **CHES1-Ri-7** | 6,948 | - | 6,968 | Open Biosystems | shRNA Clone V2HS_176180 |
| **CHES1-Ri-8** | 7,036 | - | 7,056 | Open Biosystems | shRNA Clone V2HS_176181 |
| **CHES1-Ri-9** | 7,137 | - | 7,157 | Open Biosystems | shRNA Clone V2HS_176182 |

**Figure 9.** Location of sites targeted by CHES1-specific shRNAs. ***A)*** The *CHES1* mRNA (7,856 bases) is schematically represented. The CDS (green) is indicated as well as the locations of the sites targeted by shRNAs (Ri-1, -2. etc.) used in our experiments. ***B)*** The shRNAs used in this study were either custom-designed to target the CHES1 CDS or were purchased from Open Biosystems. The information for each shRNA is presented in this table, including name, specific location, source, and clone number (if applicable).

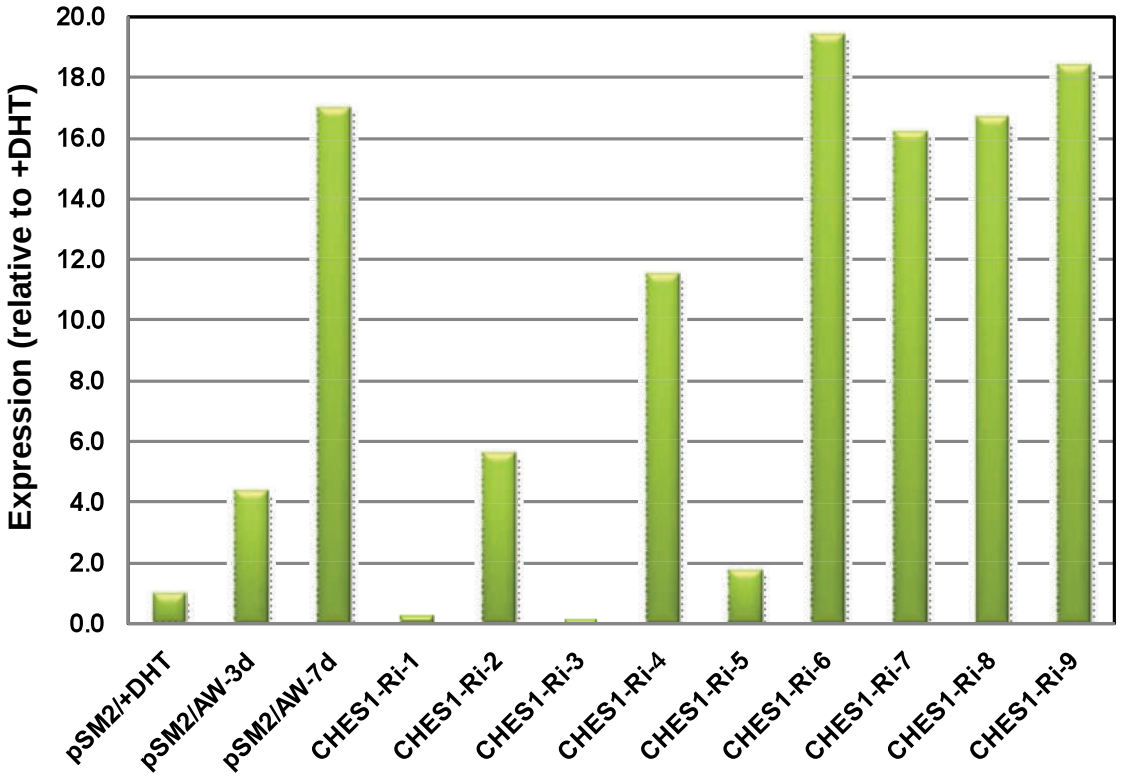


**Figure 10.** Functional validation of *CHES1*-targeting shRNA expression constructs. Retroviruses were generated from pSM2 shRNA expression constructs (and empty vector) by transfection into LinX-A packaging cells, followed by incubation at 32℃ for three days, and then harvesting of the viral supernatant. LNCaP sub-lines stably-integrated with each indicated shRNA expression construct were generated by antibiotic selection with puromycin. LNCaP-pSM2/empty cells were incubated in the presence of DHT (1 nM) or subjected to AW for 3 and 7 days **(*pSM2/AW-3d, -7d*)**. All LNCaP-pSM2-*CHES1*-Ri sublines were androgen-deprived for 7 days. RNA was then isolated and the expression of CHES1 assayed by qRT-PCR. Expression was normalized to *GAPDH* levels and relative fold changes calculated by comparison to CHES1 levels in the LNCaP-pSM2 subline cultured in the presence of androgen.

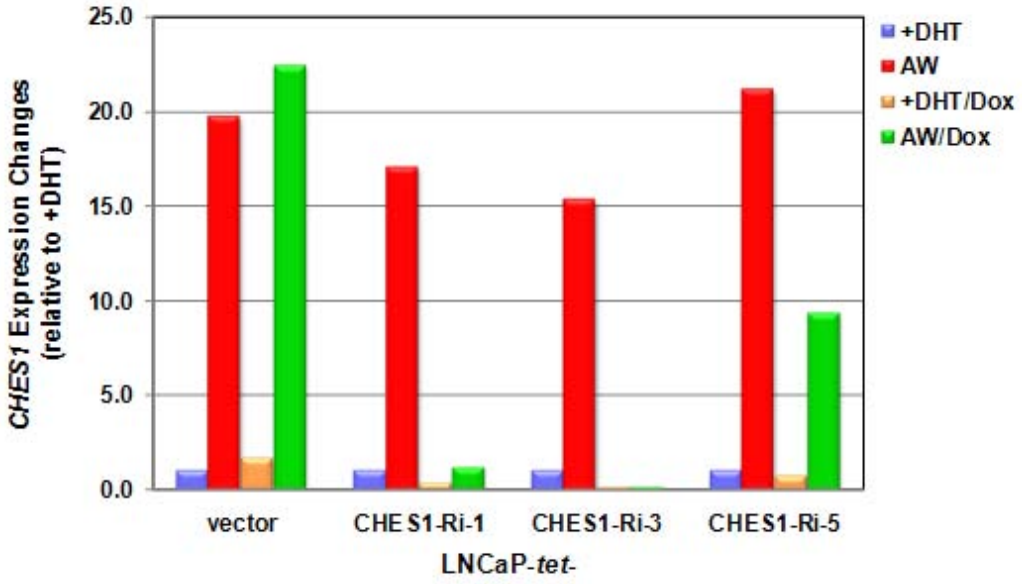


**Figure 11.** Characterization of LNCaP sublines having inducible *CHES1* shRNA expression. The previous experiment demonstrated that the most potent shRNA constructs were CHES1-Ri-1, -3, and -5. In order to generate a conditionally-inducible shRNA model, the shRNA-encoding sequences were moved from pSM2 into the tetracycline/doxycycline (Dox)-regulated pTRIPZ lentivector. Lentiparticles for each pTRIPZ-CHES1-Ri were then produced by co-transfection into HEK293 cells with the TransLenti Viral Packaging System (Open Biosystems). LNCaP cells were infected with each pTRIPZ-CHES1-Ri viral vector and then selected and maintained by incubation in the presence of puromycin. The condiional of the system was then tested . Each tetracycline/doxycycline-regulated LNCaP subline **(LNCaP-*tet*-)** was cultured in the presence of androgen **(*DHT*)** or subjected to androgen withdrawal **(*AW*)** alone or in combination with doxycycline (***Dox***; 500 µg/ml) for 7 days. RNA was isolated and *CHES1* expression evaluated by qRT-PCR as described in the legend to Figure 10. Relative *CHES1* expression changes in response to each treatment were calculated based upon comparison to the DHT-treated (without Dox) sample from each subline.